receptor (GRs), in bone have been identified mainly in osteoblasts and bone marrow cells.[4,5] The transcriptional activities of the receptors are mediated by interaction with several classes of coactivators/corepressors in a ligand-dependent manner.[11,12] The first characterized steroid receptor coactivator (SRC) family contains three homologous members: SRC-1, SRC-2 (also known as TIF2 and GRIP1), and SRC-3 (also known as p/CIP, AIB1, RAC3, ACTR, and TRAM-1).[13–16] The SRC coactivators have been reported to function in several ways: recruitment of histone acetyltransferases, histone methyltransferases, interaction with other coactivators, and contact with certain general transcription factors.[13] There are several pieces of evidence that the SRC coactivators play important roles clinically in mediating the response to steroid hormones. A chromosomal translocation that involves SRC-2 was identified in acute myeloid leukemia.[17] SRC-3 overexpression was documented in breast, ovarian, and pancreatic cancer.[18,19] These data suggest the possibility that the SRC family could modulate the response to steroid hormones in bone as well.

SRC-1 was originally cloned as a strong transactivator of GR[14] and has been reported to enhance the actions of many nuclear receptors, including ERs and AR.[13] Clinical involvement of SRC-1 has not yet been found; however, its in vivo function has been investigated by analyses of the *SRC-1*–deficient mice created by the O'Malley group using a conventional gene targeting method.[20] There were no apparent abnormalities in their major organs except for a partial resistance to sex hormones and thyroid hormone.[20–23] Aiming at generating double/triple mutant mice with tissue-specific *SRC-1* deficiency and other cofactor gene mutations such as SRC-2 and SRC-3 without embryonic lethality in the future, we first created floxed *SRC-1* mice in which the SRC-1 gene locus was flanked by loxP sites. In this study, the first using the floxed mice, we generated *SRC-1*–deficient ($SRC\text{-}1^{-/-}$) mice, whose SRC-1 function was generally blocked, by mating them with CMV-Cre transgenic mice. To define the functions of SRC-1 in skeletal tissues of both males and females, we analyzed the bone phenotype of the $SRC\text{-}1^{-/-}$ mice under physiological conditions and under stimulation by estrogens, androgens, or glucocorticoids.

MATERIALS AND METHODS

Generation of SRC-$1^{-/-}$ *mice*

Mouse SRC-1 genomic clones were obtained by screening an embryonic stem (ES) cell genomic library in λ phage (Stratagene) using human SRC-1 cDNA as a probe. A 20-kb fragment of mouse SRC-1 containing exons 3–5, encoding the basic-helix-loop-helix (bHLH) domain, was used to construct the targeting vector (Fig. 1A). The targeting vector consisted of a 7.7-kb 5′ homologous region containing exon 4, a 3.3-kb 3′ homologous region, a single loxP site, and the phosphoglycerate kinase-neomycin (PGKneo) cassette between the two loxP sites. The linearized targeting vector was electroporated into ES cells (25 μg/1.0 × 10^7 cells) using a Gene Pulser II (Bio-Rad Laboratories) at 250 V and 500 μF, and G418 neomycin-resistant clones were expanded as described previously.[24] Two ES cell clones (Fig. 1B, 4p29 and 4q30) containing a targeted *SRC-1L3* allele were identified by Southern blot analysis of *Eco*RI-digested ES cell genomic DNA, using 5′ (probe 1) and 3′ (probe 2) external probes and a neomycin probe. Targeted ES cells were aggregated with single eight-cell embryos from ICR mice (CLEA Japan) and returned to a pseudopregnant host of the same strain to generate chimeras as described previously.[24] Chimeric males were crossed with C57BL/6J females (CLEA Japan) to produce germ line transmission of the targeted *L3* allele. $SRC\text{-}1^{L3/L3}$ mice were then crossed with the CMV-Cre transgenic mice to generate $SRC\text{-}1^{L-/+}$ (also designated as $SRC\text{-}1^{+/-}$) mice (mice bearing one allele in which exon 4 and the neomycin cassette were deleted). Inbreeding of $SRC\text{-}1^{L-/+}$ mice yielded $SRC\text{-}1^{L-/L-}$ (also designated as $SRC\text{-}1^{-/-}$) mice homozygous for the deletion of SRC-1 exon 4. Because $SRC\text{-}1^{L3/L3}$ mice and CMV-Cre transgenic mice were in different strains, all $SRC\text{-}1^{-/-}$ mice used in this study had been backcrossed for 10 generations into the C57BL/6 background.

Animal conditions

All mice were kept in plastic cages under standard laboratory conditions with a 12-h dark, 12-h light cycle and a constant temperature of 23°C and humidity of 48%. The mice were fed a standard rodent diet (CE-2; CLEA Japan) containing 25.2% protein, 4.6% fat, 4.4% fiber, 6.5% ash, 3.44 kcal/g, 2.5 IU vitamin D_3/g, 1.09% calcium, and 0.93% phosphorus with water ad libitum. In each experiment, homozygous wildtype (WT) and $SRC\text{-}1^{-/-}$ mice that were littermates generated from the intercross between heterozygous mice were compared. All experiments were performed according to the protocol approved by the Animal Care and Use Committee of the University of Tokyo.

RT-PCR analysis

Total RNA was extracted from excised femora and tibias using an ISOGEN kit (Wako Pure Chemical Industries) and reverse transcribed using XL reverse transcriptase (Takara Shuzo Co.) and an oligo (dT) primer (Takara Shuzo Co.). After first-strand cDNA synthesis, 5% of the reaction mixture was amplified with r-*Taq*DNA polymerase (Takara Shuzo Co.) using specific primer pairs: 5′-CATGTAGGCCATGAGG TCCACCAC-3′ and 5′-TGAAGGTCGGTGTGAACGGATTTGGC-3′ for G3PDH; 5′-TACTGAGAAGAGGCGCAGGG-3′ and 5′-CCAGAAGAAGAGGGCCCAGC-3′ for SRC-1 (exon 4-exon 5); and 5′-ATGAGTGGCCTTGGGGACAG-3′ and 5′-CCAGAAGAAGAGGGCCCAGC-3′ for SRC-1 (exon 3-exon 5). Up to 35 cycles of amplification were performed, with each cycle consisting of 96°C for 30 s, 55°C for 60 s, and 72°C for 60 s.

Western blot analysis

To detect SRC-1 protein expression, bone cell lysates were separated by SDS-PAGE and transferred onto nitrocellulose membranes. Membranes were probed with a goat polyclonal antibody raised against a carboxyl terminus peptide of human SRC-1 that is identical to the corresponding mouse sequence (1:1000 dilution, C-20; Santa Cruz Biotechnology) and a rabbit polyclonal antibody raised against a recombinant protein corresponding to amino acids 350–

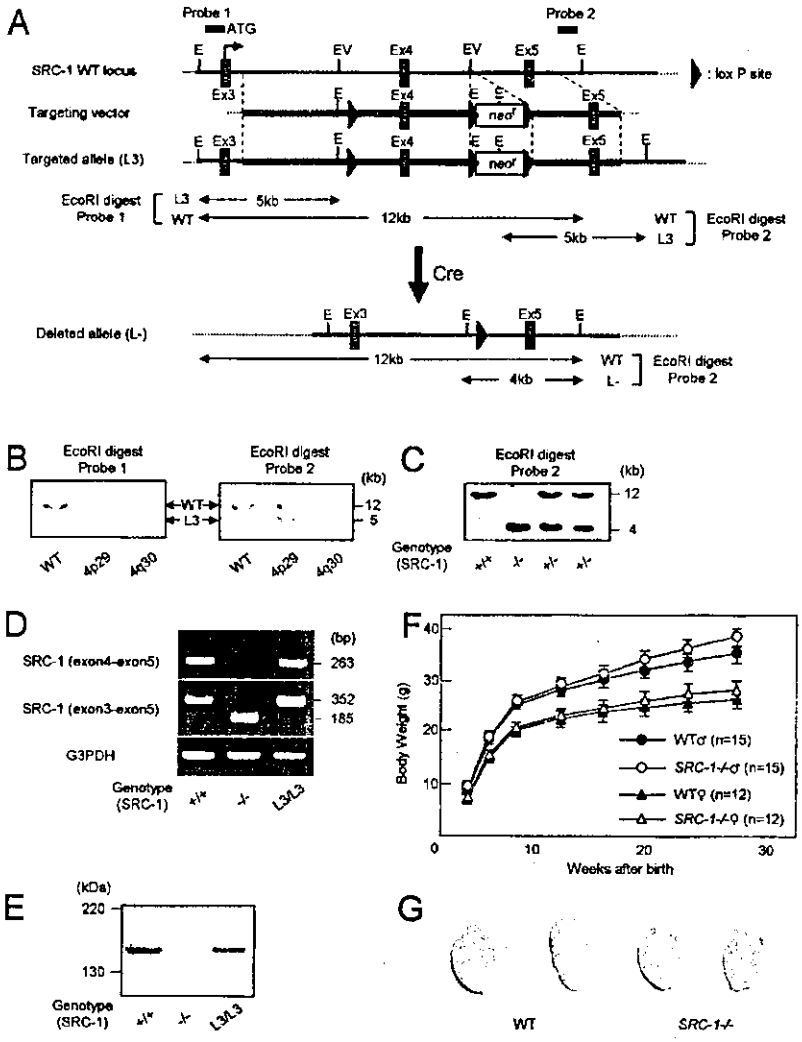

FIG. 1. Targeted disruption of mouse *SRC-1* gene. (A) Strategy to generate *SRC-1*$^{-/-}$ mice showing the WT SRC-1 locus, the targeting vector, the targeted allele (*L3*), and the deleted allele (*L*−) obtained after Cre-mediated excision. Exons (Ex) are shown as shaded boxes. The location of probes 1 and 2 are indicated. E, *Eco*RI; EV, *Eco*RV; neo^r, PGKneo cassette. LoxP sites are indicated as black arrowheads. (B) Southern blot analysis of targeted ES clones. Genomic DNA from WT ES cells and homologous targeted clones (4p29 and 4q30) were digested with *Eco*RI for hybridization with probe 1 (left) and 2 (right). (C) Southern blot analysis of offspring of heterozygous mates with probe 2. (D) Detection of the SRC-1 transcript by RT-PCR in long bones of WT, *SRC-1*$^{-/-}$, and floxed *SRC-1* (*SRC-1*$^{L3/L3}$) mice. (E) Western blot analysis of the SRC-1 protein using an antibody against a carboxyl terminus of the SRC-1 peptide in long bones of WT, *SRC-1*$^{-/-}$, and floxed *SRC-1* (*SRC-1*$^{L3/L3}$) mice. (F) Growth curves determined by the body weight of WT and *SRC-1*$^{-/-}$ mice in both sexes. Data are expressed as means (symbols) ± SE (error bars) for 15 mice/group for males and 12 mice/group for females. There were no significant differences between WT and *SRC-1*$^{-/-}$ mice in either sex ($p > 0.05$). (G) Smaller testes were observed in male *SRC-1*$^{-/-}$ mice.

690 mapping within an internal region of SRC-1 of mouse origin (1:1000 dilution, M-341; Santa Cruz Biotechnology) and then a peroxidase-conjugated second antibody. Blots were visualized using an ECL detection kit (Amersham Biosciences).

Radiological analysis

Bone radiographs of excised femora, tibias, and the fifth lumbar vertebrae from 12-, 16-, and 24-week-old WT and *SRC-1*$^{-/-}$ littermates were taken using a soft X-ray apparatus (model CMB-2; SOFTEX). BMD was measured by DXA using a bone mineral analyzer (PIXImus Mouse Densitometer; GE Medical Systems). CT was performed with a pQCT analyzer (XCT Research SA+; Stratec Medizintecnik) operating at a resolution of 80 μm. Metaphyseal pQCT scans of femora were performed to measure the trabecular volumetric BMD. The scan was positioned in the metaphysis at 1.2 mm proximal from the distal growth plate. This area contains cortical as well as trabecular bone. The trabecular bone region was defined by setting the threshold to 395 mg/cm^3 according to a previous report.[25] Mid-diaphyseal pQCT scans of femora were performed to determine the cortical volumetric BMD and the cortical thickness. The mid-diaphyseal region of femora in mice contains mostly cortical bone. The cortical bone region was defined by setting the threshold to 690 mg/cm^3.[25] The interassay CVs for the pQCT measurements were <2%. μCT scanning of the fifth lumbar vertebrae was performed using a composite X-ray analyzer (model NX-CP-C80H-IL; Nittetsu ELEX Co.), and a total of 300 cross-sectional tomograms per vertebra were obtained with a slice thickness of 10 μm and reconstructed at 12 × 12 pixels into a 3D feature by the volume-rending method (software, VIP-Station; Teijin System Technology) using a computer (model SUN SPARK-5; Sun Microsystems). Electronic sections were cut in the transverse, coronal, and sagittal planes on 3D reconstructed images.

Histological analysis

Histological analyses were performed using 24-week-old WT and *SRC-1*$^{-/-}$ littermates. For von Kossa and toluidine blue stainings, lumbar vertebrae were fixed with 70% ethanol, embedded in glycol methacrylate without decalcification, and sectioned in 3-μm slices using a microtome (model 2050; Reichert Jung). For calcein double labeling,

mice were injected subcutaneously with 16 mg/kg body weight of calcein at 10 and 3 days before death. Sections with toluidine blue stainings were used to visualize calcein labels under fluorescent light microscopy. $TRACP^+$ cells were stained at pH 5.0 in the presence of L(+)-tartaric acid using naphthol AS-MX phosphate (Sigma-Aldrich Co.) in *N,N*-dimethyl formamide as the substrate. The specimens were subjected to histomorphometric analyses using a semi-automated system (Osteoplan II; Carl Zeiss), and measurements were made at 400× magnification. Parameters for the trabecular bone were measured in an area 0.3 mm in length from the cortical bone at the fifth lumbar vertebrae. Nomenclature, symbols, and units are those recommended by the Nomenclature Committee of the American Society for Bone and Mineral Research.[26]

Serum and urinary biochemistry

Blood samples from 24-week-old WT and *SRC-1*$^{-/-}$ littermates (n = 15/genotype for males and n = 12/genotype for females) were collected by heart puncture under Nembutal (Dainippon Pharmaceutical Co.) anesthesia, and urine samples were collected for 24 h before death using oil-sealed bottles in metabolism cages (CL-0305; CLEA Japan). The levels of calcium, phosphorus, and alkaline phosphatase activity in serum were measured using a calcium HR kit (Wako Pure Chemical Industries), an inorganic phosphorus II kit (Wako Pure Chemical Industries), and a liquitech alkaline phosphatase kit (Roche Diagnostics), respectively, with an autoanalyzer (type 7170; Hitachi Hith-Technologies). Serum osteocalcin levels were measured using the competitive radioimmunoassay (RIA) kit (Biomedical Technologies). Serum testosterone and 17β-estradiol (E_2) levels were measured using RIA kits (Diagnostic Products), and serum leptin was assayed with the ELISA-based Quantikine M mouse leptin immunoassay kit (R&D Systems). Urinary deoxypyridinoline was measured using the Pyriliks-D ELISA (Metra Biosystems). The values were corrected according to urinary creatinine (Cr), as measured by a standard colorimetric technique with an autoanalyzer (type 7170).

Gonadectomy and hormone treatment

Male WT and *SRC-1*$^{-/-}$ littermates were orchidectomized or sham-operated at 16 weeks of age and implanted subcutaneously with 60-day time-release pellets (Innovative Research of America) containing either placebo or 5α-dihydrotestosterone (DHT; 10 mg/pellet; 8 mice/group). Female WT and *SRC-1*$^{-/-}$ littermates were ovariectomized or sham-operated at 16 weeks of age and implanted subcutaneously with 60-day time-release pellets containing either placebo or E_2 (0.025 mg/pellet; 8 mice/group). For the glucocorticoid experiment, male WT and *SRC-1*$^{-/-}$ littermates were implanted subcutaneously with 60-day time-release pellets containing either placebo or prednisolone (4 mg/pellet) at 16 weeks of age (8 mice/group). BMD of the fifth lumbar vertebrae was measured in situ by DXA using a bone mineral analyzer (PIXImus Mouse Densitometer) at 16 and 24 weeks. All mice were killed at 24 weeks of age, seminal vesicles of male and uteri of female mice were excised and weighed, and BMD of the excised fifth lumbar vertebrae was measured by DXA.

Statistical analysis

All data are expressed as means ± SE. Means of groups were compared by ANOVA, and significance of differences was determined by posthoc testing using Bonferroni's method.

RESULTS

Generation of SRC-1$^{-/-}$ *mice by a Cre-loxP system*

We targeted exon 4 of the *SRC-1* gene, which encodes the bHLH domain to generate functionally null SRC-1 mutant mice (Fig. 1A). The targeting vector was designed with three loxP sites flanking exon 4 and the PGKneo cassette. Complete excision of exon 4 and floxed PGKneo cassette in the *L3* allele mediated by Cre recombinase was confirmed in the genomic DNA sequence of F_2 offspring, and the mutation resulted in the creation of a stop codon at exon 5 by splicing exon 3 and 5 transcripts. Thus, the truncated protein produced from the deleted allele lacks the C-terminal region that includes all SRC-1 functional domains for transcriptional activation, histone acetyltransferase activity, and interactions with nuclear receptors, CBP, P300, and p/CAF.[14,27,28]

Chimeric males derived from targeted L3 ES clones transmitted the mutation through their germline, yielding floxed *SRC-1* (*SRC-1*$^{L3/L3}$) mice. Floxed *SRC-1* mice grew normally and exhibited no overt abnormalities with normal SRC-1 mRNA and protein expression levels (Figs. 1D and 1E). Floxed *SRC-1* mice were crossed with CMV-Cre transgenic mice to generate SRC-1 heterozygous (*SRC-1*$^{+/-}$) mice. Inbreeding of heterozygous *SRC-1*$^{+/-}$ mice yielded *SRC-1*$^{-/-}$ mice in accordance with Mendelian expectations (Fig. 1C). Short SRC-1 transcripts exclusive of exon 4 were detected by RT-PCR in the long bones of *SRC-1*$^{-/-}$ mice (Fig. 1D); however, because of the creation of a stop codon at exon 5, no SRC-1 protein expression was shown by Western blot analysis using an antibody against a carboxyl terminus of the SRC-1 peptide, confirming disruption of the *SRC-1* gene (Fig. 1E). Similar mRNA and protein expression patterns were observed in tissues including liver, kidney, isolated primary osteoblasts, and bone marrow cells, even when we used other primer sets and antibodies (data not shown).

Both male and female *SRC-1*$^{-/-}$ mice grew normally and were apparently indistinguishable from WT littermates. Growth curves determined by the body weight were somewhat similar between WT and *SRC-1*$^{-/-}$ mice in both males and females during the observation period up to 28 weeks, although a slight increase of body weight caused by obesity was seen in both sexes of *SRC-1*$^{-/-}$ mice as they got older (Fig. 1F). While no abnormality of reproductive organs, including ovary and uterus, was found in female *SRC-1*$^{-/-}$ mice, a slight hypoplasia of testis was seen (~20% in weight) in males (Fig. 1G). These abnormalities were the same as those reported in the *SRC-1*–deficient mice generated by a conventional method.[20]

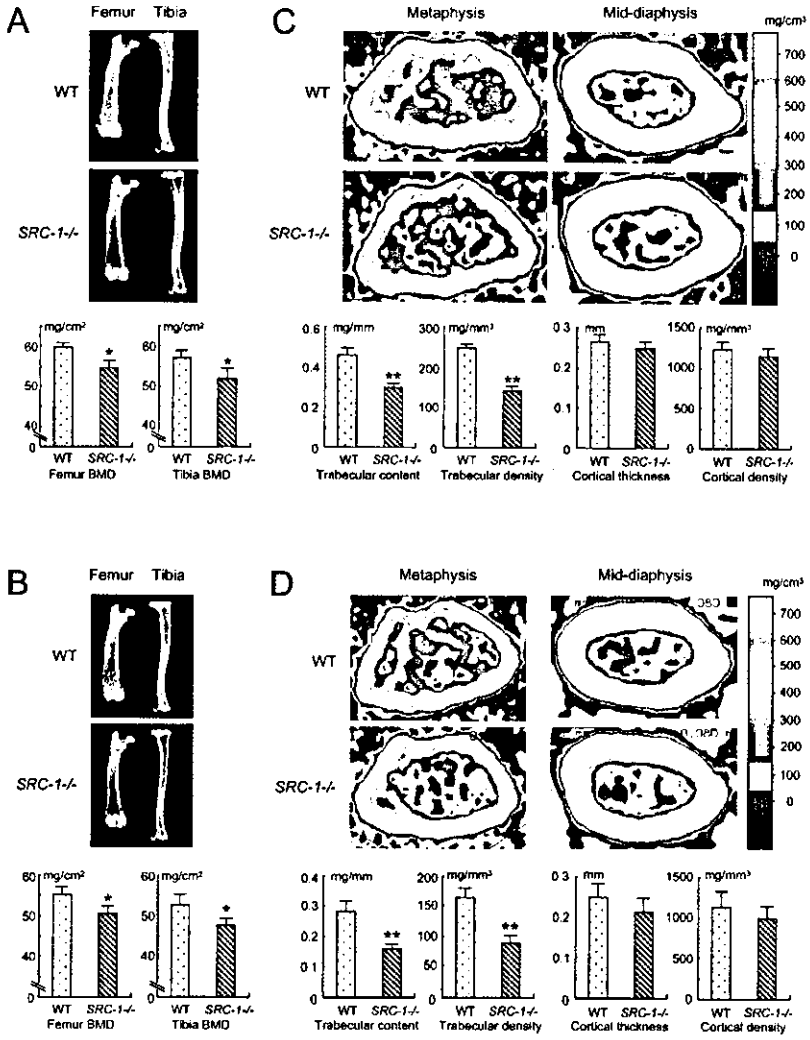

FIG. 2. Radiological findings of the long bones in *SRC-1*$^{-/-}$ and WT littermates. (A and B) Plain X-ray images of femur and tibia in representative (A) males and (B) females of both genotypes at 24 weeks of age. The BMD of the entire femurs and tibias measured by DXA is shown in the graphs below. (C and D) pQCT images of the distal metaphysis (left) and the mid-diaphysis (right) of the femurs in representative (C) males and (D) females of both genotypes at 24 weeks of age. The color gradient indicating BMD is shown in the right bars. The trabecular content and density at the metaphysis and the cortical thickness and density at the mid-diaphysis are shown in the graphs below. Data in all graphs are expressed as means (bars) ± SE (error bars) for 15 mice/group for males and 12 mice/group for females. Significant difference from WT: $*p < 0.05$, $**p < 0.01$.

Osteopenia in male and female SRC-1$^{-/-}$ *mice*

To learn the physiological role of SRC-1 in skeletal tissues, we analyzed the long bones and vertebrae of *SRC-1*$^{-/-}$ mice. The lengths of the long bones and the trunk of these mice were similar to those of WT littermates, at least during the observation period up to 24 weeks of age, indicating that SRC-1 is not involved in the regulation of skeletal growth. BMD was similar between long bones of the two genotypes at 12 weeks of age and tended to be lower in *SRC-1*$^{-/-}$ than WT mice at 16 weeks, although this was not statistically significant (data not shown). At 24 weeks, however, *SRC-1*$^{-/-}$ mice showed ~10% less BMD of long bones than WT littermates in males (Fig. 2A) and females (Fig. 2B). When trabecular and cortical bones were analyzed separately in the femora using pQCT, *SRC-1*$^{-/-}$ mice showed ~35–45% lower BMC and BMD of trabecular bones; however, the cortical bones were not affected by the SRC-1 deficiency in either males (Fig. 2C) or females (Fig. 2D).

To investigate the abnormalities of the *SRC-1*$^{-/-}$ trabecular bones in more detail, we performed morphological analyses of vertebral bodies that are rich in trabecular bone in males and females at 24 weeks of age. 3D CT analysis of the fifth lumbar vertebrae confirmed the decrease in *SRC-1*$^{-/-}$ trabecular bone in both sexes (Fig. 3).

Histomorphometric analyses confirmed that the bone volumes (BV/TV) were decreased by 30–40% in the *SRC-1*$^{-/-}$ males and females compared with those of WT littermates (Table 1). Parameters for both bone formation (Ob.S/BS, MAR, and BFR) and resorption (N.Oc/B.Pm, Oc.S/BS, and ES/BS) were also significantly higher in *SRC-1*$^{-/-}$ mice. The increase in bone resorption parameters (~60–80%) exceeded that in bone formation parameters (~30–60%), indicating a state of high-turnover osteopenia that is characteristic of osteoporosis with sex hormone deficiency.

Biochemical markers in the serum and urine supported the increase of bone turnover by SRC-1 deficiency (Table 2). Bone formation markers (serum alkaline phosphatase and osteocalcin) and a bone resorption marker (urinary deoxypyridinoline) were higher in both males and females of *SRC-1*$^{-/-}$ mice than those in WT littermates. The serum calcium and phosphorus levels were similar between the two genotypes, suggesting that the skeletal abnormalities by SRC-1 deficiency were not the result of the changed calcium or phosphorus levels. Considering that *SRC-1*$^{-/-}$ mice

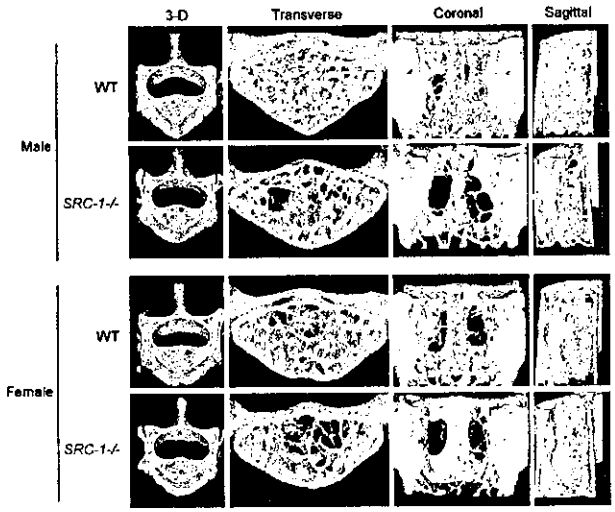

FIG. 3. Radiological and histological findings of the lumbar vertebrae in *SRC-1*$^{-/-}$ and WT littermates. 3D CT images of the fifth vertebrae in representative males and females of both genotypes at 24 weeks of age. The BMD of the entire fifth vertebrae measured by DXA was 58.7 ± 3.5 (male WT), 49.0 ± 2.1 (male *SRC-1*$^{-/-}$), 48.7 ± 3.3 (female WT), and 41.6 ± 1.4 mg/cm^2 (female *SRC-1*$^{-/-}$) for 15 mice/group for males and 12 mice/group for females. There were significant differences between WT and *SRC-1*$^{-/-}$ in both sexes ($p < 0.05$).

showed a slight obesity at this age, we measured the serum level of leptin, which has recently been reported to be an antiosteogenic factor. The level was somewhat upregulated, although not significantly, in *SRC-1*$^{-/-}$ mice. Interestingly, despite the high bone turnover, the serum levels of both testosterone in males and estradiol in females were elevated in *SRC-1*$^{-/-}$ mice, suggesting a compensatory mechanism in the endocrine system for the insensitivity to these sex hormones.

Insensitivity to administration of sex hormones in gonadectomized SRC-1$^{-/-}$ *mice*

To examine the involvement of SRC-1 in the skeletal actions of sex hormones, we performed hormone administration experiments (Figs. 4A–4D). After orchidectomy and ovariectomy on males and females, respectively, at 16 weeks of age, a slow-releasing pellet of sex hormone or placebo was subcutaneously implanted, and BMD was measured at 24 weeks. Effects of gonadectomies and hormone replacements were confirmed by seminal vesicle and uterine weights of males and females, respectively (Table 3). Both orchidectomy and ovariectomy markedly decreased these weights in WT and *SRC-1*$^{-/-}$ mice. DHT and E_2 restored them to the levels similar to those of sham-operated mice in WT, whereas these hormones restored almost one-half of them in *SRC-1*$^{-/-}$ mice, which is consistent with a previous study using another *SRC-1* knockout mouse.[20] Regarding BMD, besides the raw BMD values (Figs. 4A and 4C), the percent changes from baseline to final BMD during 8 weeks (Figs. 4B and 4D) were also compared between WT and *SRC-1*$^{-/-}$ mice. Both orchidectomy and ovariectomy decreased bone volumes of the two genotypes to the same levels in both sexes (~45.0 mg/cm^2 in males and 38.5 mg/cm^2 in females). When slow-releasing pellets of DHT and E_2 were subcutaneously implanted in the gonadectomized males and females, respectively, they prevented bone loss in WT mice. However, these hormone replacements restored little of the bone loss in *SRC-1*$^{-/-}$ mice, indicating that SRC-1 deficiency impairs the skeletal responses to sex hormones in both males and females.

We further examined the contribution of SRC-1 to the catabolic action of glucocorticoids on bone (Figs. 4E and 4F). When a slow-releasing pellet of prednisolone was implanted at 16 weeks, BMD was reduced similarly in WT and *SRC-1*$^{-/-}$ littermates, ~10% during the following 8 weeks, suggesting that SRC-1 is not essential in the bone catabolic action of glucocorticoids mediated by GR.

DISCUSSION

In this study, we originally generated *SRC-1*$^{-/-}$ mice by means of a Cre-loxP system and confirmed the lack of *SRC-1* gene expression in bone and other tissues. There is another *SRC-1* knockout mouse line that was generated by the O'Malley group, using a conventional gene targeting method.[20] Because both our *SRC-1*$^{-/-}$ mice and the conventional *SRC-1* knockout mice have similar genetic backgrounds by being extensively backcrossed into C57BL/6, we assume that the two mice should exhibit similar phenotypes. Modder et al.[29] recently reported skeletal phenotypes of the conventional *SRC-1* knockout mice showing resistance to the osteoanabolic action of estradiol in ovariectomized females, which is consistent with our results. Comparison of the two knockout mice is summarized in Table 4. In the conventional knockout mice, the targeting event inserted an in-frame stop codon at the Met (381) in exon 11, causing the downstream deletion of genomic sequence. Although the RNA encoding the bHLH-PAS domain was normally expressed in the knockout mice, all SRC-1 functional domains for transcriptional activation were confirmed to be disrupted, and it was not likely to have a dominant negative effect, because the bHLH-Per-Arnt-Sim (PAS) domain interacted with neither the full-length SRC-1 nor other SRC-1 family members such as TIF2.[20] In our *SRC-1*$^{-/-}$ mice, a stop codon created in the middle of the bHLH-PAS domain at exon 5 predicts a truncated product that is shorter than that in the conventional *SRC-1* knockout mice. Besides the skeletal finding in female mice in the previous report,[29] this study revealed that the SRC-1 deficiency also caused resistance to osteoanabolic action of androgen in orchidectomized males and no abnormality in osteocatabolic action of glucocorticoids. Discrepancy between the previous and present studies seems to be the bone phenotype under physiological conditions: their conventional *SRC-1* knockout mice did not exhibit osteopenia, whereas our *SRC-1*$^{-/-}$ mice did. We believe, however, that this discrepancy is caused by the difference in age when the analyses were done: 12 weeks for them versus 24 weeks for us. In fact, our study also did not detect significant difference of BMD at 12 weeks between WT and *SRC-1*$^{-/-}$ littermates of either sex under physiological conditions. It is speculated that, with aging, the compensatory elevation of

TABLE 1. HISTOMORPHOMETRY OF TRABECULAR BONE OF LUMBAR VERTEBRAE

	BV/TV (%)	*Ob.S/BS (%)*	*MAR (μm/day)*	*BFR (μm³/μm²/day)*	*N.Oc/B.Pm (/100 mm)*	*Oc.S/BS (%)*	*ES/BS (%)*
Male							
WT	16.48 ± 2.09	6.27 ± 0.63	0.94 ± 0.19	0.08 ± 0.02	94.24 ± 11.31	2.10 ± 0.15	3.45 ± 0.49
SRC-1$^{-/-}$	11.53 ± 1.39*	9.15 ± 0.81*	1.40 ± 0.15*	0.13 ± 0.02	159.05 ± 12.02†	3.50 ± 0.21†	5.73 ± 0.57†
Female							
WT	12.97 ± 0.65	8.55 ± 0.51	1.02 ± 0.11	0.11 ± 0.01	109.66 ± 12.64	2.41 ± 0.19	3.72 ± 0.25
SRC-1$^{-/-}$	7.73 ± 0.95†	11.02 ± 1.32	1.42 ± 0.08*	0.18 ± 0.03*	174.95 ± 24.39*	4.28 ± 0.31†	6.47 ± 0.21†

Parameters for the trabecular bone were measured in an area 0.3 mm in length from cortical bone at the fifth lumbar vertebrae in toluidine blue and calcein double-labeled sections. Data are expressed as means ± SEM (n = 15/group for males and n = 12/group for females). BV/TV, trabecular bone volume expressed as a percentage of total tissue volume; Ob.S/BS, percentage of bone surface covered by cuboidal osteoblasts; MAR, mineral apposition rate; BFR, bone formation rate expressed by MAR × percentage of bone surface exhibiting double labels plus one half single labels; N.Oc/B.Pm, number of mature osteoclasts in 10 cm of bone perimeter; Oc.S/BS, percentage of bone surface covered by mature osteoclasts; ES/BS, percentage of eroded surface.
*$p < 0.05$; †$p < .01$; significantly different from WT mice.

TABLE 2. SERUM AND URINARY BIOCHEMISTRY

	Serum							*Urine*
	ALP (IU/liter)	*Osteocalcin (ng/ml)*	*Ca (mg/dl)*	*P (mg/dl)*	*Leptin (ng/ml)*	*Testosterone (ng/ml)*	*17β-estradiol (pg/ml)*	*DPD (nM/mM Cr)*
Male								
WT	78.16 ± 6.91	20.61 ± 1.76	7.93 ± 0.21	7.52 ± 0.49	6.01 ± 0.74	2.45 ± 0.33	2.34 ± 0.21	8.29 ± 0.42
SRC-1$^{-/-}$	99.67 ± 8.16*	26.42 ± 2.16*	8.11 ± 0.18*	7.51 ± 0.57	7.45 ± 0.57	3.41 ± 0.42*	2.78 ± 0.28	11.31 ± 0.1†
Female								
WT	90.22 ± 5.74	25.05 ± 1.62	8.04 ± 0.11	7.18 ± 0.29	6.87 ± 0.67	ND	5.18 ± 0.57	9.32 ± 0.19
SRC-1$^{-/-}$	117.13 ± 7.72*	33.34 ± 1.41†	7.87 ± 0.19	7.15 ± 0.41	8.18 ± 1.24	ND	7.12 ± 0.64*	12.71 ± 0.28†

Data are expressed as means ± SEM (n = 15/group for males and n = 12/group for females). *ALP*, alkaline phosphatase; *Ca*, calcium; *P*, phosphorus; *DPD*, deoxypyridinoline; ND, not detected.
Concentration of *DPD* was collected according to urinary creatinine concentration.
*$p < 0.05$; †$p < 0.01$; significantly different from WT mice.

sex hormone levels through a feedback mechanism becomes too weak to catch up with the decreased sensitivity to these hormones by the SRC-1 deficiency.

Administration experiments with steroid hormones revealed that the SRC-1 deficiency caused resistance to osteoanabolic actions of sex hormones in gonadectomized male and female mice. More interesting is that *SRC-1*$^{-/-}$ mice exhibited osteopenia under physiological conditions at 24 weeks, suggesting a bone-sparing role of endogenous SRC-1. This is also likely to be caused by the impairment of actions of endogenous sex hormones on bone for the following reasons. First, morphological and biochemical analyses revealed that *SRC-1*$^{-/-}$ mice exhibited the decrease in trabecular bone with a high turnover state, which is characteristic of the pathology of sex hormone deficiencies. Second, the serum sex hormone levels were upregulated in *SRC-1*$^{-/-}$ mice of both sexes, implicating a compensatory reaction for the insensitivity to them. Third, in the absence of sex hormones by gonadectomies, the BMD decreased to similar levels between WT and *SRC-1*$^{-/-}$ mice. These results indicate that the SRC-1 function is essential for the maintenance of bone mass by sex hormones under both physiological and pathological conditions.

In males, as well as activating the AR, androgens can be converted into estrogens by the enzyme aromatase,[30] and therefore can exert their effects not only through the AR, but also through the ERs. Because DHT cannot be converted to estrogens by aromatase, loss of the osteoanabolic effect of exogenous DHT in *SRC-1*$^{-/-}$ orchidectomized male mice can be interpreted as a defect in AR, but not ER, signaling. Furthermore, we and others recently revealed that the androgen/AR signaling is indispensable for male-type bone remodeling, independent of the estrogen/ER signaling, by the analysis of AR-deficient mice.[31,32] Under physiological conditions, however, there are many reports showing the essential contribution of the estrogen/ER signaling to male bones. Inhibition of aromatase activity in male rats impairs bone remodeling and mimics the effect of orchidectomy,[33,34] and the aromatase-deficient mice develop osteopenia.[35] Two men with mutations in the *aromatase P450* gene exhibited delayed skeletal maturation and osteopenia, despite high levels of circulating androgens and the ability to respond to estradiol.[36,37] These observations are similar to those seen in a man with a mutation in the ER,[38] reinforcing the importance of the estrogen/ER signaling in male bones. In addition, the SRC-1 transcriptional activation of AR is known to be much weaker than that of ERs.[39] Therefore, the bone loss seen in *SRC-1*$^{-/-}$ males may, at least in part, be caused by impairment of the

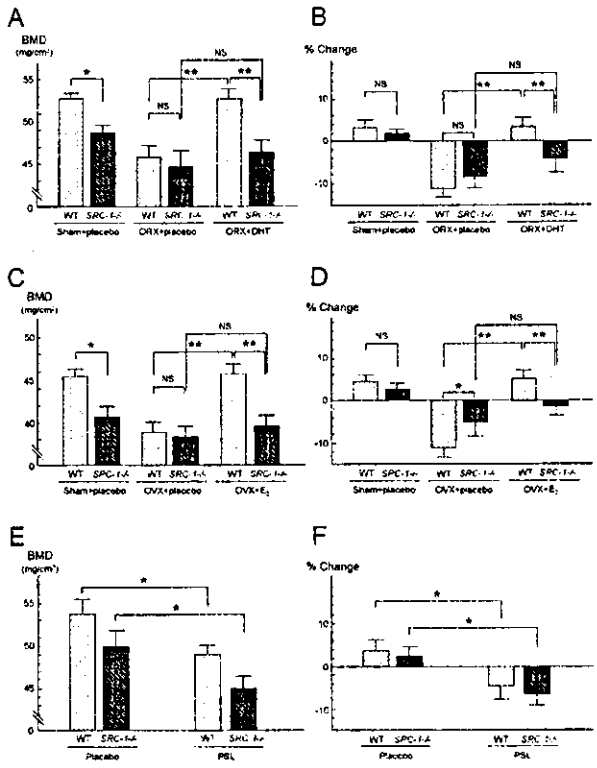

FIG. 4. Effects of gonadectomy and hormone administrations on BMD of vertebrae in *SRC-1*$^{-/-}$ and WT littermates. (A and B) Male WT and *SRC-1*$^{-/-}$ littermates were orchidectomized or sham-operated at 16 weeks of age and implanted subcutaneously with slow-releasing pellets containing either placebo or DHT (10 mg/pellet). At 16 and 24 weeks of age, BMD of the fifth lumbar vertebrae was measured by DXA. (C and D) Female WT and *SRC-1*$^{-/-}$ littermates were ovariectomized or sham-operated at 16 weeks of age and implanted subcutaneously with slow-releasing pellets containing either placebo or E_2 (0.025 mg/pellet). BMD was measured as described above. (E and F) Male WT and *SRC-1*$^{-/-}$ littermates without operation were implanted subcutaneously with slow-releasing pellets containing either placebo or prednisolone (PSL; 4 mg/pellet) at 16 weeks of age. BMD was measured as described above. Both the (A, C, and E) raw BMD values of the excised vertebrae at 24 weeks and (B, D, and F) the percent changes of BMD of the vertebrae measured in situ during 8 weeks were compared between WT and *SRC-1*$^{-/-}$ mice. Data in all graphs are expressed as means (bars) ± SE (error bars) for 8 mice/group. Significant difference: $*p < 0.05$, $**p < 0.01$. NS, not significant ($p > 0.05$).

estrogen/ER signaling, as well as of the androgen/AR signaling.

It is interesting that SRC-1 deficiency caused the decrease of trabecular bone but not of cortical bone. Similar findings are reported in a study using the conventional *SRC-1* knockout mice.[29] A previous study examining ERα and ERβ expressions by immunohistochemistry in neonatal human ribs showed that trabecular bone contains both ERs, whereas only ERα was detected in cortical bone.[40] Modder et al.[29] also showed that the cancellous bone of the mouse vertebrae contains both ERs, whereas the cortical bone of the mouse femur contains exclusively ERα. In addition, another recent study revealed that, in osteoblastic cells, SRC-1 potentiates the transcriptional activity of co-expressed ERα/ERβ or ERβ alone, with little or no potentiation of ERα.[41] Hence, as Modder et al.[29] stated in their report, at least in females, the discrepancy of the SRC-1 contribution between trabecular and cortical bone may be caused by the relative expression of ERα versus ERβ in the two kinds of bone and to the specific interactions of SRC-1 with these receptor isoforms in bone cells. In males as well, difference of effects on the two kinds of bone can be explained by the distinctions of expression and activation of the ER isoforms, because estrogen/ER signaling is important in male bone, as described above. Regarding AR, its distribution in the trabecular and cortical bones remains unknown. Further studies on the expression and the interaction with SRC-1 of AR and ERs will elucidate the clinical importance of SRC-1 in human bones.

The conventional *SRC-1* knockout mice are reported to be obesity prone under a high-fat diet.[42] In this study as well, our *SRC-1*$^{-/-}$ mice, fed a standard diet, showed higher body weight and serum leptin levels compared with those of WT littermates, although both were slight and not statistically significant. A series of recent reports showed that leptin, an anorexigenic hormone secreted by adipocytes, also shows antiosteogenic action centrally through hypothalamic and sympathetic nervous systems.[43] However, this low level of increase in the leptin level seems inadequate to explain the significant bone loss by the SRC-1 deficiency. In addition, the *SRC-1*$^{-/-}$ bone exhibited high bone turnover with stimulated bone formation, which is the opposite of leptin action.

Nuclear receptors exert their tissue-specific function using different coactivator/corepressor complexes ingeniously and appropriately in each tissue.[11,12,44] Therefore, it is possible that not only the dysfunction of nuclear receptors or their ligands, but also that of the cofactors, leads to various disorders. The function of cofactors might explain the difference among individuals in the sensitivity to hormones and related agents as well. Despite important roles of sex hormones in bone, the effect of their gain or loss of function varies widely among individuals, and this has not yet been fully explained by analyses of the receptor levels. Accumulated genetic studies have failed to identify a definite association of the ER or AR gene polymorphisms with BMD.[45] Furthermore, a case of testicular feminization in a patient without an AR gene mutation was reported as a possible co-factor disease.[46] From the results of this study, SRC-1 may be a strong candidate that regulates the variety of the pathophysiology of sex hormone-deficient osteoporosis and therapeutic effects of hormone replacements in humans, because humans are known to be more sensitive to sex hormone deficiency than mice.

ACKNOWLEDGMENTS

We thank Dr Yasuji Yamamoto (Taiho Pharmaceutical Co., Ltd.) for helpful discussion and Kaori Yamamoto (ELK Corp.) and the hard tissue research team at Kureha Chemical Industry Co., Ltd. for technical assistance. This study was supported by a Grant-in-Aid for Scientific Research from the Japanese Ministry of Education, Culture, Sports, Science, and Technology (15659348).

TABLE 3. EFFECTS OF GONADECTOMIES AND HORMONE REPLACEMENTS ON REPRODUCTIVE TISSUES

	WT			*SRC-1*$^{-/-}$		
	Sham + placebo	*Gonadectomy + placebo*	*Gonadectomy + hormone*	*Sham + placebo*	*Gonadectomy + placebo*	*Gonadectomy + hormone*
Seminal vesicle weights of males (g)	0.31 ± 0.03	0.03 ± 0.01*	0.35 ± 0.03	0.28 ± 0.03	0.03 ± 0.01*	0.18 ± 0.02†
Uterine weights of females (g)	0.12 ± 0.02	0.02 ± 0.01*	0.13 ± 0.03	0.11 ± 0.03	0.02 ± 0.01*	0.05 ± 0.02†

Data are expressed as means ± SEM (n = 8/group for males and females).
*$p < 0.01$, significantly different from the respective sham group.
†$p < 0.01$, significantly different from the respective WT mice.

TABLE 4. COMPARISON BETWEEN TWO *SRC-1*$^{-/-}$ KNOCKOUT MICE

	Modder et al.[29]	*This study*
Generation of mice		
Targeting method	Conventional	Floxed mice × CMV-Cre transgenic mice
Locus of stop codon	Exon 11	Exon 5
Genetic background	C57BL/6	C57BL/6
Physiological conditions		
Age of analysis	12 weeks	12 & 24 weeks
Skeletal phenotype		
12 weeks	Normal	Normal
24 weeks	—	Osteopenia
Hormone administration experiments		
Age	12–20 weeks	16–24 weeks
Estrogen action on females	Decreased	Decreased
Estrogen dose/pellet	15 μg/60-d & 60 μg/60-d	25 μg/60-d
Androgen action on males	—	Decreased
Glucocorticoid action on males	—	Unaffected

REFERENCES

1. Evans RM 1988 The steroid and thyroid hormone receptor superfamily. Science **240**:889–895.
2. Mangelsdorf DJ, Thummel C, Beato M, Herrlich P, Schutz G, Umesono K, Blumberg B, Kastner P, Mark M, Chambon P, Evans RM 1995 The nuclear receptor superfamily: The second decade. Cell **83**:835–839.
3. Tsai MJ, O'Malley BW 1994 Molecular mechanisms of action of steroid/thyroid receptor superfamily members. Annu Rev Biochem **63**:451–486.
4. Bland R 2000 Steroid hormone receptor expression and action in bone. Clin Sci (Lond) **98**:217–240.
5. Compston JE 2001 Sex steroids and bone. Physiol Rev **81**:419–447.
6. Bilezikian JP 2002 Sex steroids, mice, and men: When androgens and estrogens get very close to each other. J Bone Miner Res **17**:563–566.
7. Riggs BL, Khosla S, Melton LJ III 2002 Sex steroids and the construction and conservation of the adult skeleton. Endocr Rev **23**:279–302.
8. Francis RM 1999 The effects of testosterone on osteoporosis in men. Clin Endocrinol (Oxf) **50**:411–414.
9. Canalis E 1996 Clinical review 83: Mechanisms of glucocorticoid action in bone. Implications to glucocorticoid-induced osteoporosis. J Clin Endocrinol Metab **81**:3441–3447.
10. Osella G, Terzolo M, Reimondo G, Piovesan A, Pia A, Termine A, Paccotti P, Angeli A 1997 Serum markers of bone and collagen turnover in patients with Cushing's syndrome and in subjects with adrenal incidentalomas. J Clin Endocrinol Metab **82**:3303–3307.
11. Glass CK, Rosenfeld MG 2000 The coregulator exchange in transcriptional functions of nuclear receptors. Genes Dev **14**:121–141.
12. McKenna NJ, O'Malley BW 2002 Combinatorial control of gene expression by nuclear receptors and coregulators. Cell **108**:465–474.
13. Xu J, O'Malley BW 2002 Molecular mechanisms and cellular biology of the steroid receptor coactivator (SRC) family in steroid receptor function. Rev Endocr Metab Disord **3**:185–192.
14. Onate SA, Tsai SY, Tsai MJ, O'Malley BW 1995 Sequence and characterization of a coactivator for the steroid hormone receptor superfamily. Science **270**:1354–1357.
15. Hong H, Kohli K, Trivedi A, Johnson DL, Stallcup MR 1996 GRIP1, a novel mouse protein that serves as a transcriptional coactivator in yeast for the hormone binding domains of steroid receptors. Proc Natl Acad Sci USA **93**:4948–4952.
16. Voegel JJ, Heine MJ, Zechel C, Chambon P, Gronemeyer H 1996 TIF2, a 160 kDa transcriptional mediator for the ligand-dependent activation function AF-2 of nuclear receptors. EMBO J **15**:3667–3675.
17. Carapeti M, Aguiar RC, Watmore AE, Goldman JM, Cross NC 1999 Consistent fusion of MOZ and TIF2 in AML with inv(8)(p11q13). Cancer Genet Cytogenet **113**:70–72.
18. Bautista S, Valles H, Walker RL, Anzick S, Zeillinger R, Meltzer P, Theillet C 1998 In breast cancer, amplification of the steroid receptor coactivator gene AIB1 is correlated with estrogen and progesterone receptor positivity. Clin Cancer Res **4**:2925–2929.
19. Ghadimi BM, Schrock E, Walker RL, Wangsa D, Jauho A, Meltzer PS, Ried T 1999 Specific chromosomal aberrations and amplification of the AIB1 nuclear receptor coactivator gene in pancreatic carcinomas. Am J Pathol **154**:525–536.
20. Xu J, Qiu Y, DeMayo FJ, Tsai SY, Tsai MJ, O'Malley BW 1998 Partial hormone resistance in mice with disruption of the steroid receptor coactivator-1 (SRC-1) gene. Science **279**:1922–1925.
21. Weiss RE, Xu J, Ning G, Pohlenz J, O'Malley BW, Refetoff S 1999 Mice deficient in the steroid receptor co-activator 1 (SRC-1) are resistant to thyroid hormone. EMBO J **18**:1900–1904.
22. Weiss RE, Gehin M, Xu J, Sadow PM, O'Malley BW, Chambon P, Refetoff S 2002 Thyroid function in mice with compound heterozygous and homozygous disruptions of SRC-1 and TIF-2

coactivators: Evidence for haploinsufficiency. Endocrinology **143:** 1554–1557.
23. Takeuchi Y, Murata Y, Sadow P, Hayashi Y, Seo H, Xu J, O'Malley BW, Weiss RE, Refetoff S 2002 Steroid receptor coactivator-1 deficiency causes variable alterations in the modulation of T(3)-regulated transcription of genes in vivo. Endocrinology **143:**1346–1352.
24. Nakamichi Y, Shukunami C, Yamada T, Aihara K, Kawano H, Sato T, Nishizaki Y, Yamamoto Y, Shindo M, Yoshimura K, Nakamura T, Takahashi N, Kawaguchi H, Hiraki Y, Kato S 2003 Chondromodulin I is a bone remodeling factor. Mol Cell Biol **23:**636–644.
25. Ferretti JL 2000 Peripheral Quantitative Computed Tomography for Evaluating Structural and Mechanical Properties of Small Bone Mechanical Testing of Bone and the Bone-Implant Interface. CRC Press, Boca Raton, FL, USA, pp. 385–405.
26. Parfitt AM, Drezner MK, Glorieux FH, Kanis JA, Malluche H, Meunier PJ, Ott SM, Recker RR 1987 Bone histomorphometry: Standardization of nomenclature, symbols, and units. Report of the ASBMR Histomorphometry Nomenclature Committee. J Bone Miner Res **2:**595–610.
27. Heery DM, Kalkhoven E, Hoare S, Parker MG 1997 A signature motif in transcriptional co-activators mediates binding to nuclear receptors. Nature **387:**733–736.
28. Spencer TE, Jenster G, Burcin MM, Allis CD, Zhou J, Mizzen CA, McKenna NJ, Onate SA, Tsai SY, Tsai MJ, O'Malley BW 1997 Steroid receptor coactivator-1 is a histone acetyltransferase. Nature **389:**194–198.
29. Modder UI, Sanyal A, Kearns AE, Sibonga JD, Nishihara E, Xu J, O'Malley BW, Ritman EL, Riggs BL, Spelsberg TC, Khosla S 2004 Effects of loss of steroid receptor coactivator-1 on the skeletal response to estrogen in mice. Endocrinology **145:**913–921.
30. Simpson ER, Mahendroo MS, Means GD, Kilgore MW, Hinshelwood MM, Graham-Lorence S, Amarneh B, Ito Y, Fisher CR, Michael MD, Mendelson CR, Bulun SE 1994 Aromatase cytochrome P450, the enzyme responsible for estrogen biosynthesis. Endocr Rev **15:**342–355.
31. Yeh S, Tsai MY, Xu Q, Mu XM, Lardy H, Huang KE, Lin H, Yeh SD, Altuwaijri S, Zhou X, Xing L, Boyce BF, Hung MC, Zhang S, Gan L, Chang C 2002 Generation and characterization of androgen receptor knockout (ARKO) mice: An in vivo model for the study of androgen functions in selective tissues. Proc Natl Acad Sci USA **99:**13498–13503.
32. Kawano H, Sato T, Yamada T, Matsumoto T, Sekine K, Watanabe T, Nakamura T, Fukuda T, Yoshimura K, Yoshizawa T, Aihara K, Yamamoto Y, Nakamichi Y, Metzger D, Chambon P, Nakamura K, Kawaguchi H, Kato S 2003 Suppressive function of androgen receptor in bone resorption. Proc Natl Acad Sci USA **100:**9416–9421.
33. Vanderschueren D, Van Herck E, De Coster R, Bouillon R 1996 Aromatization of androgens is important for skeletal maintenance of aged male rats. Calcif Tissue Int **59:**179–183.
34. Vanderschueren D, van Herck E, Nijs J, Ederveen AG, De Coster R, Bouillon R 1997 Aromatase inhibition impairs skeletal modeling and decreases bone mineral density in growing male rats. Endocrinology **138:**2301–2307.
35. Oz OK, Zerwekh JE, Fisher C, Graves K, Nanu L, Millsaps R, Simpson ER 2000 Bone has a sexually dimorphic response to aromatose deficiency. J Bone Miner Res **15:**507–514.
36. Morishima A, Grumbach MM, Simpson ER, Fisher C, Qin K 1995 Aromatase deficiency in male and female siblings caused by a novel mutation and the physiological role of estrogens. J Clin Endocrinol Metab **80:**3689–3698.
37. Carani C, Qin K, Simoni M, Faustini-Fustini M, Serpente S, Boyd J, Korach KS, Simpson ER 1997 Effect of testosterone and estradiol in a man with aromatase deficiency. N Engl J Med **337:**91–95.
38. Smith EP, Boyd J, Frank GR, Takahashi H, Cohen RM, Specker B, Williams TC, Lubahn DB, Korach KS 1994 Estrogen resistance caused by a mutation in the estrogen-receptor gene in a man. N Engl J Med **331:**1056–1061.
39. Auger AP, Tetel MJ, McCarthy MM 2000 Steroid receptor coactivator-1 (SRC-1) mediates the development of sex-specific brain morphology and behavior. Proc Natl Acad Sci USA **97:** 7551–7555.
40. Bord S, Horner A, Beavan S, Compston J 2001 Estrogen receptors alpha and beta are differentially expressed in developing human bone. J Clin Endocrinol Metab **86:**2309–2314.
41. Monroe DG, Johnsen SA, Subramaniam M, Getz BJ, Khosla S, Riggs BL, Spelsberg TC 2003 Mutual antagonism of estrogen receptors alpha and beta and their preferred interactions with steroid receptor coactivators in human osteoblastic cell lines. J Endocrinol **176:**349–357.
42. Picard F, Gehin M, Annicotte J, Rocchi S, Champy MF, O'Malley BW, Chambon P, Auwerx J 2002 SRC-1 and TIF2 control energy balance between white and brown adipose tissues. Cell **111:**931–941.
43. Takeda S, Karsenty G 2001 Central control of bone formation. J Bone Miner Metab **19:**195–198.
44. Yanagisawa J, Kitagawa H, Yanagida M, Wada O, Ogawa S, Nakagomi M, Oishi H, Yamamoto Y, Nagasawa H, McMahon SB, Cole MD, Tora L, Takahashi N, Kato S 2002 Nuclear receptor function requires a TFTC-type histone acetyl transferase complex. Mol Cell **9:**553–562.
45. Liu YZ, Liu YJ, Recker RR, Deng HW 2003 Molecular studies of identification of genes for osteoporosis: The 2002 update. J Endocrinol **177:**147–196.
46. Adachi M, Takayanagi R, Tomura A, Imasaki K, Kato S, Goto K, Yanase T, Ikuyama S, Nawata H 2000 Androgen-insensitivity syndrome as a possible coactivator disease. N Engl J Med **343:** 856–862.

Address reprint requests to:
Hiroshi Kawaguchi, MD, PhD
Department of Orthopaedic Surgery
Faculty of Medicine
University of Tokyo
Hongo 7-3-1, Bunkyo
Tokyo 113-8655, Japan
E-mail: kawaguchi-ort@h.u-tokyo.ac.jp

Received in original form December 19, 2003; in revised form April 14, 2004; accepted May 7, 2004.

Available online at www.sciencedirect.com
SCIENCE DIRECT
Journal of Steroid Biochemistry & Molecular Biology 89–90 (2004) 627–633
The Journal of Steroid Biochemistry & Molecular Biology
www.elsevier.com/locate/jsbmb

Function of androgen receptor in gene regulations☆

Shigeaki Kato[a,b,*], Takahiro Matsumoto[a], Hirotaka Kawano[a], Takashi Sato[a], Ken-ichi Takeyama[a,b]

[a] *Institute of Molecular and Cellular Biosciences, The University of Tokyo, 1-1-1 Yayoi, Bunkyo-ku, Tokyo 113-0032, Japan*
[b] *SORST, Japan Science and Technology Corporation, 4-1-8 Honcho, Kawaguchi, Saitama 332-0012, Japan*

Abstract

Most of the androgen actions are considered to be mediated by the androgen receptor (AR) of the target genes. The AR is composed of a fairly large molecule because of the long A/B domains of its N-terminal. However, the independent roles of the AR as well as those of the estrogen receptors largely remained unknown mainly due to the lack of the AR knockout (ARKO) mice line. We have succeeded in generating the ARKO mouse by means of a conditional targeting using the Cre/loxP system. The ARKO males grew healthily although they showed a typical feature of the testicular feminization mutation (Tfm) and the hormonal assay revealed significantly lower serum androgen and higher LH levels in comparison with those of the wild type (WT) males. The serum estrogen levels were, however, comparable between both the ARKO and the WT. Another hallmark of the ARKO males was a state of high bone turnover osteopenia, in which the acceleration in the bone resorption clearly exceeded the bone formation. Male-typical behaviors were disrupted in male ARKO mice. Aiming at a quick differentiation of an androgen-dependent polyQ disease such as Kennedy's disease, the authors also developed the Drosophila fly-eye model in which the wild type and the polyQ-expanded human AR (hAR) was induced in the eyes of Drosophila. When androgen was administered to the flies induced with the polyQ-expanded hAR, their optical nerves were devastated.

Keywords: Androgen; Androgen receptor; KO mice; Transgenic fly

1. Introduction

The androgen receptor (AR), a member of the steroid hormone receptors superfamily, is composed of a fairly large protein in comparison with thyroid hormone receptors (TR), Vitamin D receptors (VDR), retinoid receptors (RXR) as well as estrogen receptors [1–3]. It is because the A/B domains of the N-terminal of the AR that include a polyQ repeat are much longer than those of other receptors [4–6]. Androgen controls the expression of genes via the AR, in which the AR positively or negatively regulates the expression of the target genes acting as androgen-dependent transcription factors, under the existence of co-activators [5–7]. When the AR functions on the DNA of the genes, the complex of the co-activators interact as a trigger with the basal transcription factor and the AR for initiating the transcription.

Recent studies of two subtypes of estrogen receptors, ERα and ERβ, found that, especially in the knockout mouse, a clear phenotypes such as osteoporosis were not manifested perhaps because the plasma level of androgen had been extremely elevated [8]. This may be explained by the fact that androgen is the precursor of estrogen in the female mouse. It has been also reported that in the aromatase knockout female mouse, the circulating testosterone levels are markedly elevated [9]. Such being the case, there was a demand in developing the androgen receptor knockout (ARKO) mouse to investigate the actions of sexual steroid hormones individually. Androgen is required for the genital organs as well as sexual behavior not only in males but also in females. And in the clinical aspect, it is well known that some prostatic cancer can be androgen-dependently aggravated. A clarification of these issues was also expected with the development of the ARKO mouse.

2. Phenotypes of androgen knockout mouse

There were basic and technical difficulties in generating an ARKO mouse. When the AR gene is mutated in the male mouse, the mouse turns out phenotypic female without having a normal female or male genitalia and is infertile [10,11]. Moreover, as the AR gene is located only

☆ Presented at the 12th Workshop on Vitamin D (Maastricht, The Netherlands, 6–10 July 2003).

* Corresponding author. Tel.: +81-3-5841-8478; fax: +81-3-5841-8477.
E-mail address: uskato@mail.ecc.u-tokyo.ac.jp (S. Kato).

0960-0760/$ – see front matter © 2004 Elsevier Ltd. All rights reserved.
doi:10.1016/j.jsbmb.2004.03.099

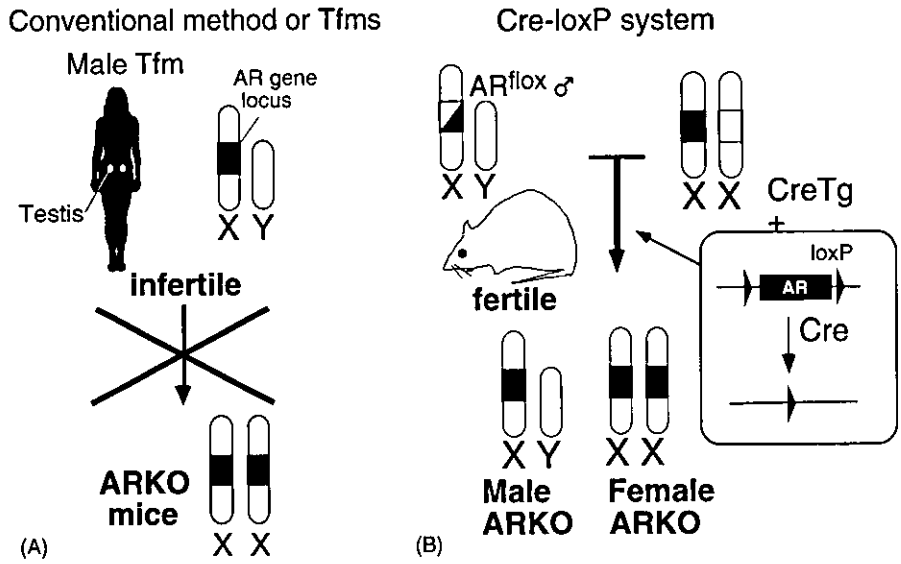

Fig. 1. Strategy for generating ARKO mice line when the male ARflox mouse with a partially modified AR gene induced by lox P and the female transgenic mouse ($CreTg^{+}$) generated by applying recombinase Cre were mated, all the AR genes were disrupted during the embryogenesis; thus, an ARKO mice line was obtained.

on the X chromosome, there is no male hetrozygoute of the AR gene-dirsrupted animals to transfer the mutated AR gene. It is thus impossible to obtain a female homozygote by either naturally occurring genetic mutaions or conventional targeted gene disruption method. Thus, the animal which has a recessive genotypic change in the AR gene can not be generated by means of the usual methods.

Such being the case, we planned to introduce the recombinase Cre/Lox-P base sequence (Cre-lox P system) into the mouse AR gene locus (Fig. 1) to generate ARKO mice line [12]. To begin with, we generated a potential AR knockout (ARKO) mouse (floxed ARf) by introducing the lox P, a capsid of a DNA breaking enzyme, in the AR gene by homologous recombination in ES cells. Three lox P sites were successively introduced in the first intron of the mouse AR gene. The male floxed AR mice are completely fertile/normal so far, and showed a normal expression and function of the AR, nevertheless, under the partially modified AR gene. On the other hand, a female transgenic mouse was generated by applying the recombinase Cre, which induces a recombination at the site between the two lox P

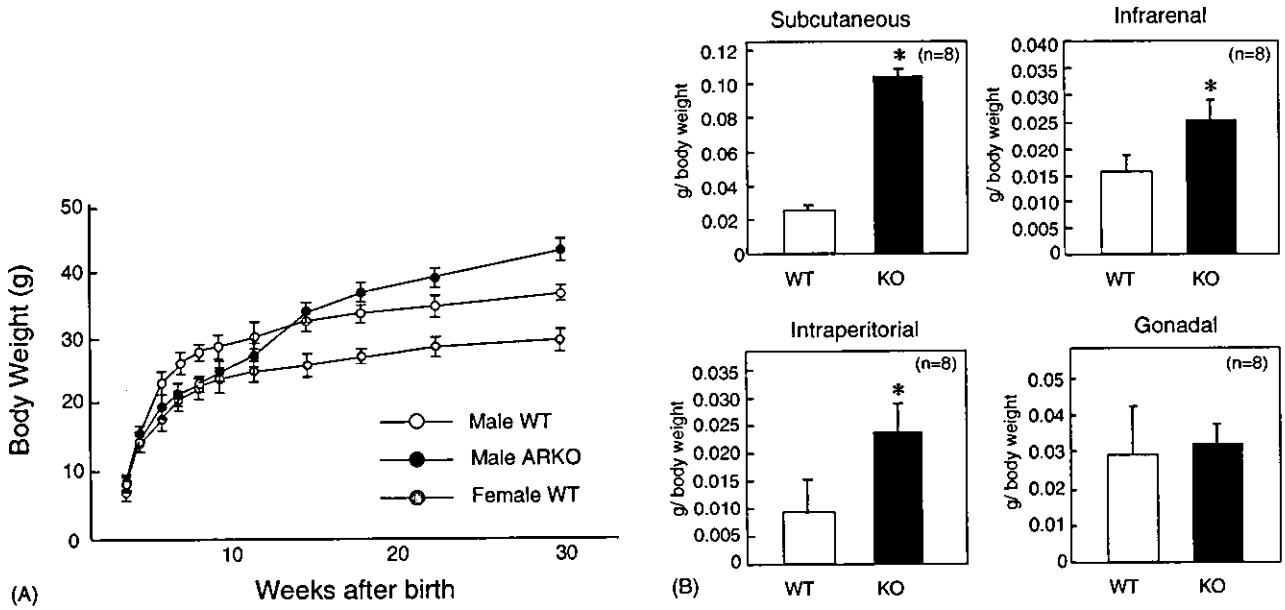

Fig. 2. Obesity in adult male ARKO mice: (A) growth curve of ARKO mice; (B) wet tissue weight of adipose tissue of male ARKO mice (Sato et. al [13]).

sequences in the same direction. Thus, in the Cre transgenic female mouse ($CreTg^+$), one of the two AR gene has been disrupted to generate the female $CreTg^+$ mice with heterozygous disruption of the AR gene. When the male floxed AR mice and these female $CreTg^+$ mice were mated, the AR gene was disrupted by expressed Cre under the CMV strong promoter during the embryogenesis.

The male ARKO which looks like a complete female had the small testes and cecum-like vagina but had no uterus and ovaries; and showed a similarity with the clinical Tfm. [13] The histological findings such as the hypertrophic Leydig cells suggested impaired spermatogenesis. The growth curves for 56 days after the birth of the female ARKO mouse (Fig. 2) were completely comparable with those of the WT female but those of the male ARKO were clearly retarded in comparison with those of the WT male and were rather similar to those of the females.

Estimation of plasma hormone levels in the male ARKO revealed markedly lowered androgens as well as a luteinizing hormone, but there was no difference in the estradiol level in comparison with that of the wild type (WT). These suggest that we can investigate the effect of androgens independently by using the ARKO mouse in that only the AR is disrupted while the estrogen receptors remain intact.

The bone densitometry showed a marked osteopenia, and the 3D-CT indicated that both of the trabecular bone and cortical bone volumes were remarkably reduced in the ARKO male mouse in comparison with that of the WT littermate male mouse at 6–16 weeks of age. Since the bone volumes result from bone remodeling which is the coupling of the formation/resorption of the bone, we compared bone formation and resorption on the proximal tibia in the ARKO and WT male by means of an histomorphometric analysis. Unexpectedly, the bone formation in the ARKO male exceeded that of the WT male by 15–20% (Fig. 3). On the

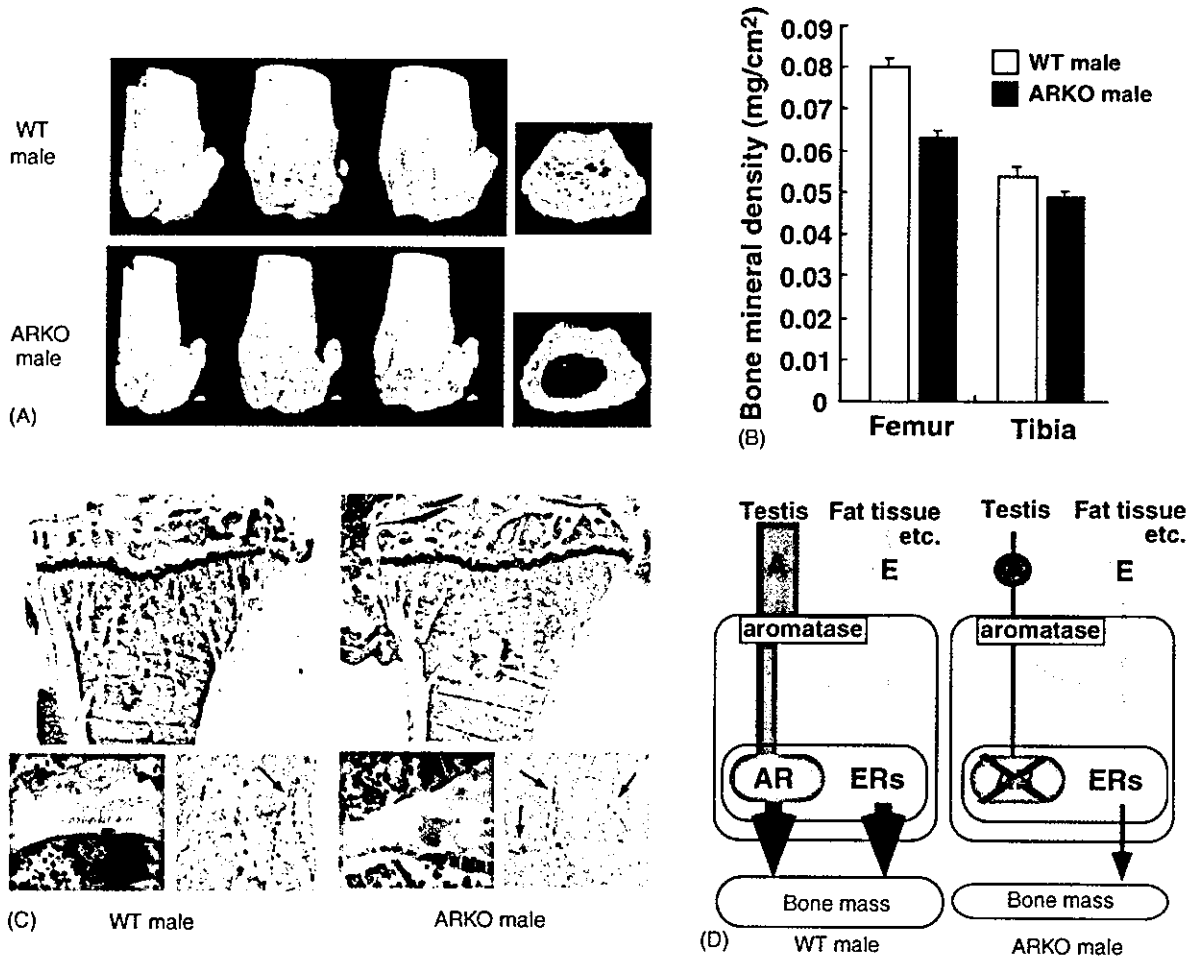

Fig. 3. Osteopenia in male ARKO mice: (A) three-dimensional CT images of distal femora and axial sections of distal metaphyses of male ARKO mice; (B) bone mineral density of male ARKO femur and tibia; (C) high turnover of male ARKO bone. Histological features and histomorphometry of the proximal tibiae from 8-week-old male ARKO and WT mice. For Villanueva-Goldner staining of sections from representative ARKO and WT male littermates, mineralized bone is stained green; (D) schema of skeletal sex hormone action. In male WT mice, skeletal sex hormone activities are mediated by both AR and ER. In female WT mice, skeletal function of ER is likely to dominate over that of AR as serum levels of AR ligands in females are quite low. In male ARKO mice, testicular testosterone production is severely impaired by hypoplasia of the testes, leading to a lack of skeletal sex hormone actions. In contrast, female ARKO mice may not be greatly affected by disruption of AR signaling.

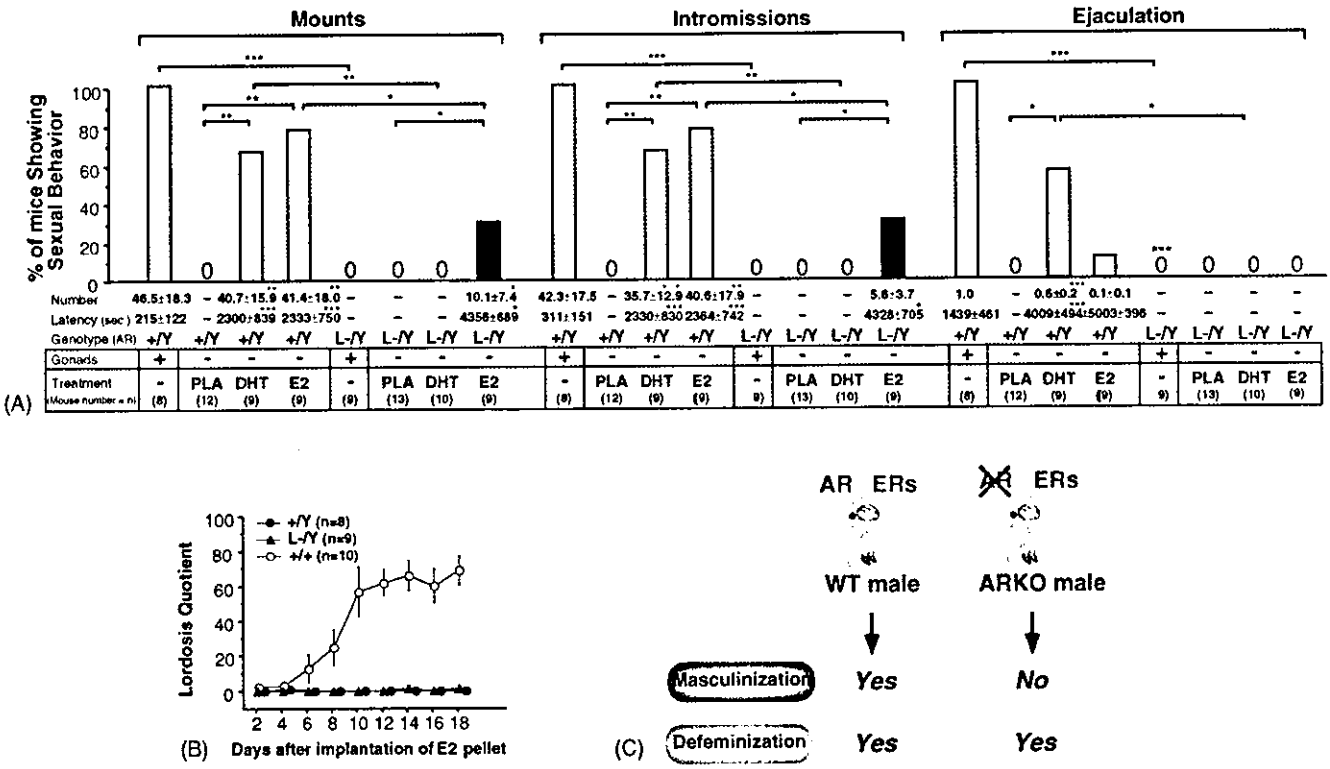

Fig. 4. Male-typical behaviors were impaired in male ARKO mice: (A) impaired male sexual behaviors in ARKO mice were partially recovered by estrogen, but not by androgen; (B) no female sexual behavior (lordosis) in male ARKO mice; (C) brain masculinization requires AR function.

other hand, the bone resorption in the ARKO male was more remarkable and exceeded that of the WT male by 40–50%. In view of these results, we concluded that the reduction in the bone found in the ARKO male was based on the high bone turnover osteopenia [14].

A characteristic change was seen in the body fat composition [13]. More than 10 weeks after the birth ARKO male became fat and the weight exceeded the normal growth curve; and the accumulation of white fat which almost doubled in comparison with the WT male was recognized under celiotomy (Fig. 2). Since there were no clear differences in serum lipids, especially in total cholesterol and free fatty acid, the AR might have suppressed the differentiation of the adipose cells. On the other hand, the sexual behavior of the ARKO mouse either as male or female was found not to be normal; nevertheless the normal gonadal differentiation was found in the ARKO female. Thus, it was considered that abnormal sexual behavior resulted in lowered number of offspring by about half of that of the WT female.

Male-typical behaviors were abolished in male ARKO mice, however, these mice showed no female sexual behavior. Estrogen treatment was effective to recover the impaired male sexual behaviors except ejaculation, suggesting that both of androgen and estrogen signalings mediated their nuclear receptors are essential for expression and maintenance of male sexual behaviors (T. Sato and T. Matsumoto, unpublished result) (Fig. 4).

3. Functional analyses of polyQ-expanded AR mutant in drosophila fly-eye model

An important disease group other than the testicular feminization mutation (Tfm) and androgen insensitivity syndrome (AIS) that is related to the mutation of the AR gene is the triplet repeat disease, or so-called polyQ expansion, in which the poly Q repetitions of the A/B domain of the N-terminal are expanded [4,5]. Spinobulbar muscular atrophy (SBMA) is one of the polyQ diseases and also named as Kennedy's disease. Other polyQ diseases such as Huntington's disease, spino-cerebellar ataxis (SCA1), and Machado-Joseph disease are seen both in males and females [15,16], while manifestation of SBMA can not be seen in the female, even if she is a carrier. Since the AF-1 functions of the A/B domain are androgen-dependent, the reason that the disease occurs only in the male was considered to be dependent on the concentration of androgen.

Aiming at proving this theory, we tried to use the Drosophila fly-eye model [17]. As the lifespan of the fly is short, we thought we could quickly obtain the assay results. The fly possesses nuclear receptors [18]. For example, it has the receptors for ecdysone, metamorphotic hormone, and its partner gene, the ultrabithorax gene. The latter is identical to the human retinoid receptor (RXR). Since the ecdysone receptor of the fly functions as a heterodimer, its DNA binding site is considered to be a direct repeat sequence; on the contrary, the DNA binding site of the human steroid

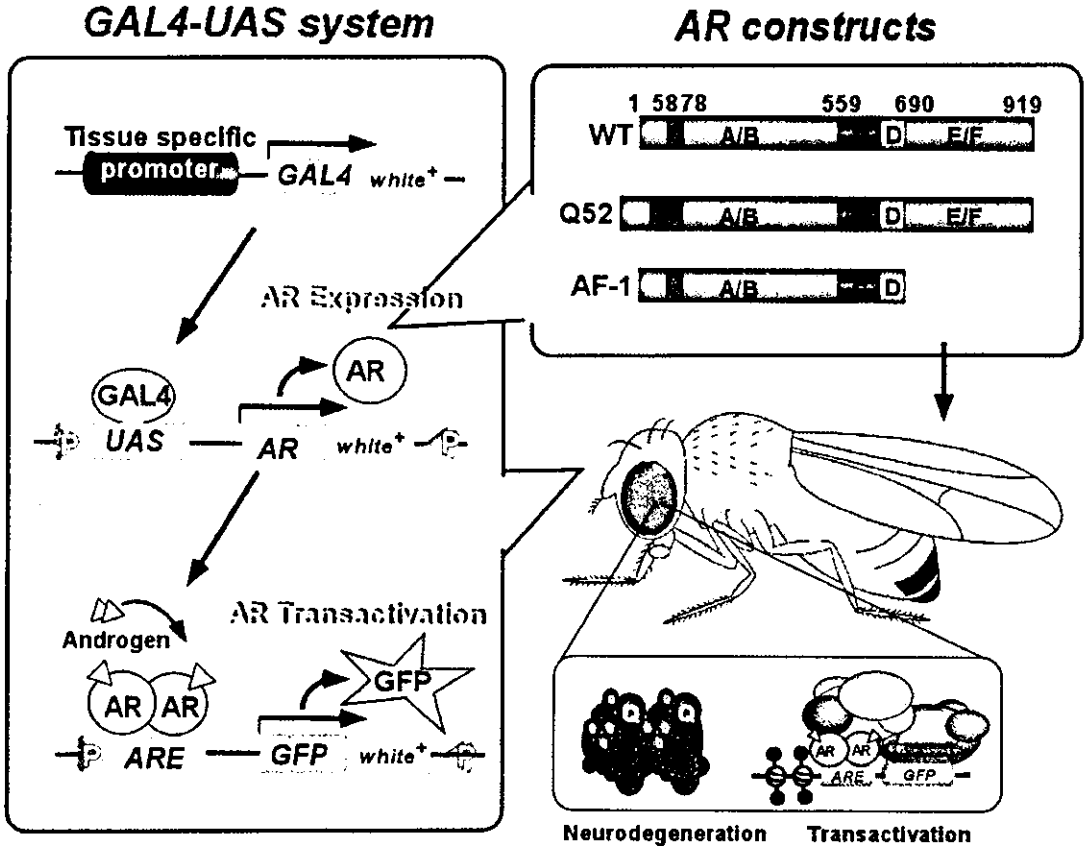

Fig. 5. Inducing hARs to the Drosophila eye, the human ARs, wild type, and polyQ-expanded, were induced in the Drosophila eyes using GAL4 UAS, then the reporter genes were bound to the GFP.

hormone receptor that functions as the homodimer is of a palindrome sequence. Such being the case, we expressed the human AR (hAR) in the fly-eye, tissue/stage specifically, using GAL4 UAS, a conditional gene expression system [19], under the expectation that this AR expression would not impair the functions of the intrinsic receptors in the fly. Then, the reporter gene, a DNA sequence, which can bind to the marker green fluorescent protein (GFP), was bound to the GFP (Fig. 5). In such a fly-eye model, the AR expression can be detected as red by staining it with the antibody; and the transcription function can be recognized as green fluorescent.

Naturally, the human AR has about 20 polyQ repetitions but when we induce too many repeat in the AR, the transcription ability is reduced and also the in vitro protein biosynthesis becomes suppressed. Consequently, we judged around 52 repetitions would be optimal for monitoring the transcription activity and the nerval death. When androgen is fed to the fly that had expressed a wild type AR (ARwt), a green fluorescent is shown in the eye without any abnormal changes. But when the polyQ repeat AR is expressed, the optical nerves (photo-receptor neurons) of the fly are devastated unless the androgen feeding is discontinued; which means the nervous system disorders are androgen-dependent. When cartinostatic agents for prostatic cancer such as hydroxy flutamide and bicalutamide are administered concomitantly, the nerve disorders of the fly were rather worsened. The results justify the development of a new-type anti-androgen for the treatment of prostatic cancer. As the AR is expressed in the nuclear and disrupts the optical nerves while keeping the transactivations, it was clarified that the disorder is based on an intranuclear event; and we recognized an androgen-dependent apoptosis was concurrently taking place.

Fig. 6 illustrates a speculation on the ligand-dependent structural alterations of the polyQ-expanded hAR [17]. The hAR that is inactive in the transactivitiy without ligand (androgen) gains transactivities under the existence of androgen by its structual alterations and also by recruiting co-activators [7,20]; while, the polyQ repeat induce apoptosis by their aggregating property. Since the plasma testosterone is much lower in the female patients (1/20–1/30), in comparison with those of the male patients, the polyQ aggregation may be difficult to occur. On the other hand, most androgen antagonists inhibit the transactivity of the AR by inhibiting recruitment of the co-activators; but they may not induce a structural alteration of the AR that deprive the aggregation by polyQ repeat. Adding finally, most of the polyQ diseases including Kennedy's disease are of late onset; and the disorders in the gonadal function and skeletal muscles appear after middle age. And on the other hand, the sensitivity of the fly-eye in expressing the polyQ repeat AR slightly changes depending on the stage.

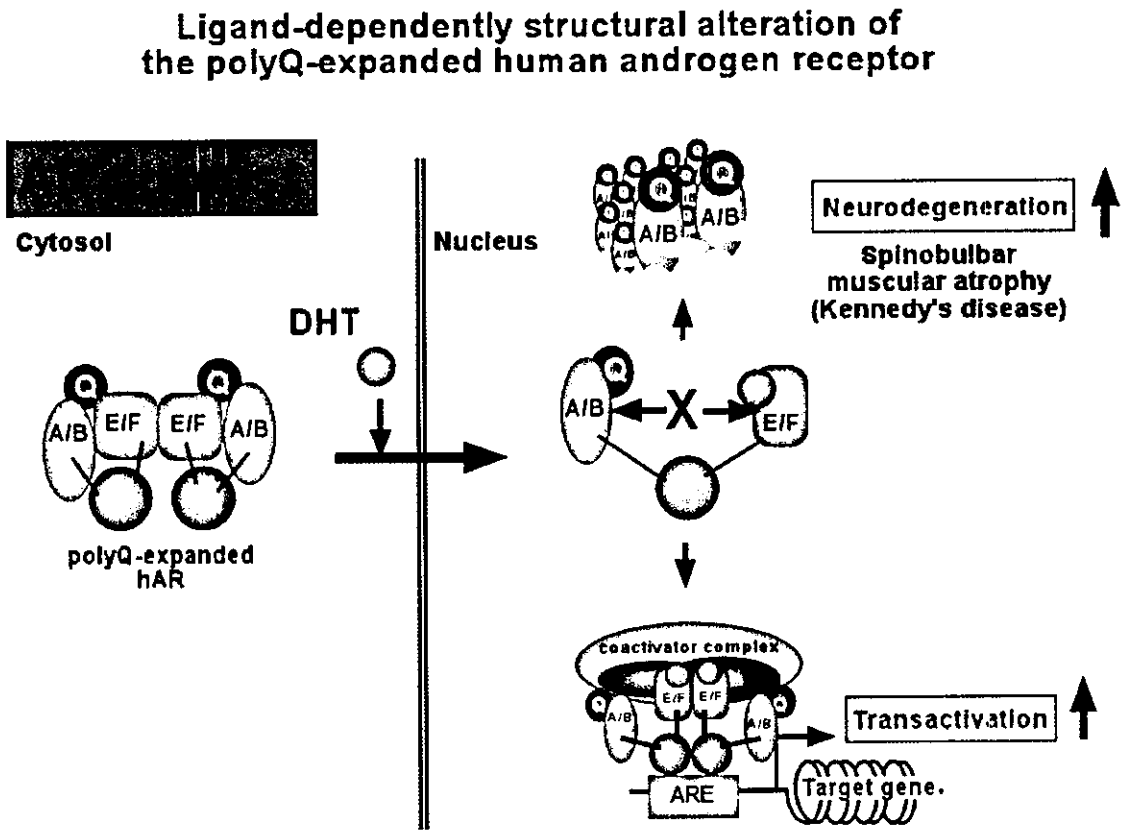

Fig. 6. Androgen-dependent structural alteration by the polyQ-expanded hAR. It is considered that the polyQ-expanded AR is inactive in the transactivation without the agonists (androgens); but under the existence of the agonists, it alters the molecular structure and also recruits the co-activators, while the polyQ repeat induces apoptosis by their aggregation.

In view of these results, we consider that for the management of Kennedy's disease, an anti-androgen treatment, such as an orchidectomy or the development of a new ligand that induces a structural alteration of the polyQ-expansion, may be required.

References

[1] M. Beato, P. Herrlich, G. Schutz, Steroid hormone receptors: many actors in search of a plot, Cell 83 (1995) 851–857.
[2] D.J. Mangelsdorf, C. Thummel, M. Beato, P. Herrlich, G. Schutz, K. Umesono, B. Blumberg, P. Kastner, M. Mark, P. Chambon, et al., The nuclear receptor superfamily: the second decade, Cell 83 (1995) 835–839.
[3] P. Chambon, A decade of molecular biology of retinoic acid receptors, FASEB J. 10 (1996) 940–954.
[4] C.S. Choong, E.M. Wilson, Trinucleotide repeats in the human androgen receptor: a molecular basis for disease, J. Mol. Endocrinol. 21 (1998) 235–257.
[5] A.R. La Spada, E.M. Wilson, D.B. Lubahn, A.E. Harding, K.H. Fischbeck, Androgen receptor gene mutations in X-linked spinal and bulbar muscular atrophy, Nature 352 (1991) 77–79.
[6] C.K. Glass, M.G. Rosenfeld, The coregulator exchange in transcriptional functions of nuclear receptors, Genes Dev. 14 (2000) 121–141.
[7] A. Yamamoto, Y. Hashimoto, K. Kohri, E. Ogata, S. Kato, K. Ikeda, M. Nakanishi, Cyclin E as a coactivator of the androgen receptor, J. Cell Biol. 150 (2000) 873–880.
[8] J.F. Couse, K.S. Korach, Estrogen receptor null mice: what have we learned and where will they lead us? [published erratum appears in Endocr. Rev. 1999 Aug 20(4):459], Endocr. Rev. 20 (1999) 358–417.
[9] C.R. Fisher, K.H. Graves, A.F. Parlow, E.R. Simpson, Characterization of mice deficient in aromatase (ArKO) because of targeted disruption of the cyp19 gene, Proc. Natl. Acad. Sci. U.S.A. 95 (1998) 6965–6970.
[10] R. Balducci, P. Ghirri, T.R. Brown, S. Bradford, A. Boldrini, B. Boscherini, F. Sciarra, V. Toscano, A clinician looks at androgen resistance, Steroids 61 (1996) 205–211.
[11] C.A. Quigley, A. De Bellis, K.B. Marschke, M.K. el-Awady, E.M. Wilson, F.S. French, Androgen receptor defects: historical, clinical, and molecular perspectives, Endocr. Rev. 16 (1995) 271–321.
[12] S. Kato, Androgen receptor structure and function from knock-out mouse, Clin. Pediatr. Endocrinol. 11 (2002) 1–7.
[13] T. Sato, T. Matsumoto, T. Yamada, T. Watanabe, H. Kawano, S. Kato, Late onset of obesity in male androgen receptor-deficient (ARKO) mice, Biochem. Biophys. Res. Commun. 300 (2003) 167–171.
[14] H. Kawano, T. Sato, T. Yamada, T. Matsumoto, K. Sekine, T. Watanabe, T. Nakamura, T. Fukuda, K. Yoshimura, T. Yoshizawa, K. Aihara, Y. Yamamoto, Y. Nakamichi, D. Metzger, P. Chambon, K. Nakamura, H. Kawaguchi, S. Kato, Suppressive function of androgen receptor in bone resorption, Proc. Natl. Acad. Sci. U.S.A. 100 (2003) 9416–9421.
[15] C.A. Ross, Intranuclear neuronal inclusions: a common pathogenic mechanism for glutamine-repeat neurodegenerative diseases? Neuron 19 (1997) 1147–1150.

[16] T.W. Kim, R.E. Tanzi, Neuronal intranuclear inclusions in polyglutamine diseases: nuclear weapons or nuclear fallout? Neuron 21 (1998) 657–659.
[17] K. Takeyama, S. Ito, A. Yamamoto, H. Tanimoto, T. Furutani, H. Kanuka, M. Miura, T. Tabata, S. Kato, Androgen-dependent neurodegeneration by polyglutamine-expanded human androgen receptor in Drosophila, Neuron 35 (2002) 855–864.
[18] K.P. White, P. Hurban, T. Watanabe, D.S. Hogness, Coordination of Drosophila metamorphosis by two ecdysone-induced nuclear receptors, Science 276 (1997) 114–117.
[19] A.H. Brand, N. Perrimon, Targeted gene expression as a means of altering cell fates and generating dominant phenotypes, Development 118 (1993) 401–415.
[20] M. Watanabe, J. Yanagisawa, H. Kitagawa, K. Takeyama, S. Ogawa, Y. Arao, M. Suzawa, Y. Kobayashi, T. Yano, H. Yoshikawa, Y. Masuhiro, S. Kato, A subfamily of RNA-binding DEAD-box proteins acts as an estrogen receptor alpha coactivator through the N-terminal activation domain (AF-1) with an RNA coactivator, SRA, Embo. J. 20 (2001) 1341–1352.

MOLECULAR AND CELLULAR BIOLOGY, July 2004, p. 6525–6535 Vol. 24, No. 14
0270-7306/04/$08.00+0 DOI: 10.1128/MCB.24.14.6525–6535.2004

Transcriptional Coactivator PC4 Stimulates Promoter Escape and Facilitates Transcriptional Synergy by GAL4-VP16

Aya Fukuda,[1]† Tomoyoshi Nakadai,[1] Miho Shimada,[1] Tohru Tsukui,[1] Masahito Matsumoto,[1] Yasuhisa Nogi,[1] Michael Meisterernst,[2] and Koji Hisatake[1]*

Department of Molecular Biology, Saitama Medical School, Moroyama, Iruma-gun, Saitama 350-0495, Japan,[1] and Gene Expression, Institute of Molecular Immunology, GSF-National Research Center for Environment and Health, Munich, Germany[2]

Received 24 December 2003/Returned for modification 18 January 2004/Accepted 14 April 2004

Positive cofactor 4 (PC4) is a coactivator that strongly augments transcription by various activators, presumably by facilitating the assembly of the preinitiation complex (PIC). However, our previous observation of stimulation of promoter escape in GAL4-VP16-dependent transcription in the presence of PC4 suggested a possible role for PC4 in this step. Here, we performed quantitative analyses of the stimulatory effects of PC4 on initiation, promoter escape, and elongation in GAL4-VP16-dependent transcription and found that PC4 possesses the ability to stimulate promoter escape in response to GAL4-VP16 in addition to its previously demonstrated effect on PIC assembly. This stimulatory effect of PC4 on promoter escape required TFIIA and the TATA box binding protein-associated factor subunits of TFIID. Furthermore, PC4 displayed physical interactions with both TFIIH and GAL4-VP16 through its coactivator domain, and these interactions were regulated distinctly by PC4 phosphorylation. Finally, GAL4-VP16 and PC4 stimulated both initiation and promoter escape to similar extents on the promoters with three and five GAL4 sites; however, they stimulated promoter escape preferentially on the promoter with a single GAL4 site. These results provide insight into the mechanism by which PC4 permits multiply bound GAL4-VP16 to attain synergy to achieve robust transcriptional activation.

Transcription of mRNA-coding genes involves RNA polymerase II and six general transcription factors (TFIIA, TFIIB, TFIID, TFIIE, TFIIF, and TFIIH) which comprise the basal transcription machinery that recognizes the core promoter elements and elicits the basal level of transcription (50). Activated transcription requires the binding of activators to the regulatory DNA sequences typically present upstream of the core promoter and their interactions with the general transcription machinery (32, 49). Despite the well-documented direct interactions of activators with the general transcription factors and RNA polymerase II, activated transcription requires yet another group of transcription factors, termed mediators or coactivators, that confer on the general transcription machinery a markedly enhanced responsiveness to activators (2, 18, 20, 36, 41).

A wide array of coactivators may be grouped into two broad categories according to the requirement of chromatin for their action in biochemical assays. The coactivators which function on the templates without chromatin include the TATA box binding protein-associated factors (TAFs) present in TFIID (58), positive cofactors (PCs) (PC1, PC2, PC3, and PC4) derived from the upstream factor stimulatory activity (USA) cofactor fraction (20), and metazoan multiprotein complexes that are structurally related to the yeast mediator (40) (TRAP/SMCC, ARC, DRIP, NAT, murine mediator, human mediator, CRSP, and PC2) (36, 41). The coactivators which require chromatin templates for their functions include CBP/p300, PCAF and its related GCN5 proteins, and p160 family proteins that display histone acetyltransferase activities (4, 65). Given their structural complexity and diversity, these coactivators are expected to show not only redundancy and cooperativity but activator and promoter selectivity as well, posing significant challenges for complete understanding of the various mechanisms by which coactivators facilitate transcription.

One way to approach the mechanisms of coactivator functions is to employ a well-defined transcription system that supports activated transcription in response to the smallest possible numbers of activators and coactivators and to identify the steps of transcription that are targeted physically and functionally by the activators and coactivators. A system well suited for this minimalist approach would be the transcription system that allows activated transcription in response to GAL4-VP16 or other GAL4-derivatives in the presence of coactivator PC4. PC4 is a coactivator that was initially identified in the USA fraction that enhances transcription by various transcriptional activators in vitro (13, 27, 38) and turned out to be identical to the 15-kDa single-stranded DNA (ssDNA)-binding protein. Although PC4 possesses both ssDNA- and double-stranded DNA (dsDNA)-binding activities, which are important for transcriptional repression, only its dsDNA-binding activity appears to correlate with the coactivator activity (62, 63). The coactivator activity of PC4 and its interaction with activators, but not the ssDNA-binding activity, are lost upon phosphorylation of the serine residues within its N-terminal region by casein kinase II (14, 27).

* Corresponding author. Mailing address: Department of Molecular Biology, Saitama Medical School, 38 Morohongo, Moroyama, Iruma-gun, Saitama 350-0495, Japan. Phone: 81-49-276-1490. Fax: 81-49-294-9751. E-mail: kojihisa@saitama-med.ac.jp.

† Present address: Laboratory of Biochemistry and Molecular Biology, The Rockefeller University, New York, NY 10021.

Since PC4 interacts with both transcriptional activators and TFIIA (13, 16) and also with TFIIB in the case of its yeast homolog, SUB1/TSP1 (16, 23), PC4 is proposed to promote the assembly of the preinitiation complex (PIC) (13, 21, 27) in activated transcription. However, given that transcription is a multistep process consisting of PIC assembly, promoter opening, initiation, promoter escape, elongation, and reinitiation, steps other than PIC assembly are potential targets for regulation as well. Indeed, despite predominant effects of activators—presumably in conjunction with coactivators—on PIC assembly, the effects on the subsequent steps (1, 28, 31, 37) have also been demonstrated in various systems, including promoter opening (60), promoter escape (10, 29), elongation (66), and reinitiation (26, 67). However, the relative contributions of activators and coactivators in stimulating individual steps of transcription remain to be more clearly defined.

In this study, we have systematically analyzed the stimulatory effects of GAL4-VP16 and PC4 and assigned their quantitative contributions to the stimulation of individual steps of transcription. Our results show that PC4 contributed to the stimulation of promoter escape as well as initiation in the presence of GAL4-VP16 and that these effects were contingent upon the presence of TFIIA and TAFs in TFIID. Consistent with the previously demonstrated requirement of the ERCC3 helicase activity of TFIIH in stimulating promoter escape (10), PC4 was found to interact specifically with TFIIH through its coactivator domain, a region that also interacted with GAL4-VP16. Furthermore, the number of GAL4 sites (and thus the number of bound GAL4-VP16 dimers) on the promoter influenced the degree of stimulation of each step by PC4, revealing possible links between the physical interactions involving PC4 and their functional consequences on the steps of transcription. Together, these results provide important clues as to the mechanism by which PC4 assists GAL4-VP16 in transcriptional activation.

MATERIALS AND METHODS

DNA templates for in vitro transcription. DNA templates pG1HMC2AT and pG3HMC2AT were created by replacement of the five GAL4-binding sites of pG5HMC2AT with the annealed oligonucleotides. The following synthetic oligonucleotides were used for one and three GAL4-binding sites: 5′-AATTCGA GCTCGGTACCAGGGGACTAGAGTCTCCGCTCGGAGGACAGTACTCC GACCTGCA-3′ and 5′-GGTCGGAGTACTGTCCTCCGAGCGGAGACTCT AGTCCCCTGGTACCGAGCTCG-3′, respectively, for pG1HMC2AT and 5′-AATTCGAGCTCGGTACCAGGGGACTAGAGTCTCCGCTCGGAGGACA GTACTCCGCTCGGAGGACAGTACTCCGCTCGGAGGACAGTACTC CGACCTGCA-3′ and 5′-GGTCGGAGTACTGTCCTCCGAGCGGAGTACTG TCCTCCGAGCGGAGTACTGTCCTCCGAGCGGAGACTCTAGTCCCCTGG TACCGAGCTCG-3′, respectively, for pG3HMC2AT. The mixtures of the complementary oligonucleotides were denatured at 90°C for 5min and were then cooled slowly to room temperature in 10 mM Tris-HCl (pH 8.0)–1 mM EDTA–50 mM NaCl. Then, the annealed oligonucleotides were used to replace the EcoRI-PstI fragment encompassing the five GAL4-binding sites of pG5HMC2AT. The obtained DNA templates were sequenced completely on both strands to rule out the possibility of spurious mutations.

Purification of transcription factors and in vitro transcription assays. Purification of recombinant factors (TFIIA, TFIIB, TFIIE, TFIIF, TFIIH, and GAL4-VP16), epitope-tagged TFIID, and RNA polymerase II were performed as described previously (10, 12). Recombinant PC4 was purified as described previously (11). For 390- and 20-nucleotide (nt) transcripts, in vitro transcription reaction mixtures (25 μl) contained 50 ng of negatively supercoiled pG5HMC2AT or its derivative, 12 mM HEPES-KOH (pH 7.9), 6% glycerol, 60 mM KCl, 0.6 mM EDTA, 8 mM $MgCl_2$, 5 mM dithiothreitol (DTT), 20 U of RNase inhibitor (TaKaRa), 0.2 mM ATP, 0.2 mM UTP, 0.1 mM 3′-*o*-methyl GTP, 12.5 μM CTP, 10 μCi of [α-^{32}P]CTP, 20 ng of TFIIA, 10 ng of TFIIB, 1 μl of FLAG-tagged TFIID (which corresponds to ~0.1 ng of TATA binding protein [TBP]), 10 ng of TFIIE, 20 ng of TFIIF, 20 ng of recombinant TFIIH, and 100 ng of RNAPII. Where indicated, the reaction mixtures contained 25 ng of GAL4-VP16 and 200 ng of PC4 as well. Transcription reactions for the initiation product were performed as described previously (10), and the derived pppApC was treated with calf intestinal phosphatase to form ApC before electrophoresis (29). After electrophoresis, the transcripts were quantified by using a Fujix Bas2000 bioimaging analyzer. Stimulation of promoter escape (*n*-fold) was calculated by dividing the stimulation of the 20G transcript (*n*-fold) by that of ApC. Similarly, stimulation of elongation (*n*-fold) was calculated by dividing the stimulation of the 390-nt transcript (*n*-fold) by that of the 20G transcript.

Preparation of PC4-GST. The coding region of PC4 was amplified by PCR with the primers 5′-GGCCTCTAGACATATGCCTAAATCAAAGG-3′ and 5′-GGCCGGATCCCAGCTTTCTTACTGCGTC-3′, which both incorporated XbaI and NdeI sites at the 5′ end and a BamHI site in place of the stop codon at the 3′ end. After digestion with XbaI and BamHI, the XbaI-BamHI fragment was subcloned into pBluescript II KS(−) (Stratagene) that was digested with XbaI and BamHI to create pBKS(−)-PC4. Then, the coding region of *Schistosoma japonicum* glutathione *S*-transferase (GST) was amplified by PCR from expression vector pGEX2TL(+) by using the primers 5′-GGCCGGATCCCCT ATACTAGGTTATTG-3′ and 5′-GGCCGGATCCAGATCTCAGTCAGTCA TTTTGGAGGATGGTCGCC-3′, which both incorporated a BamHI site at the 5′ end and BglII and BamHI sites at the 3′ end. The amplified PCR product was digested with BamHI, and the derived BamHI-BamHI fragment was inserted into the BamHI site of pBKS(−)-PC4 to create pBKS(−)-PC4-GST. After confirmation of its DNA sequence, the entire PC4-GST coding region was cut out with NdeI and BglII digestion and inserted into the NdeI and BamHI sites of pET3a (TaKaRa). PC4 deletion mutants, either as GST-PC4 or as PC4-GST, were created by using the same strategy and were inserted into the same expression vectors in place of wild-type PC4.

Recombinant GST-PC4 and PC4-GST and their derivatives were expressed in *Escherichia coli* BL21(DE3) p*Lys*S at 30°C for 3 h, and the extract was prepared by sonication in buffer C (20 mM HEPES-KOH [pH 7.9], 10% glycerol, 1 mM EDTA, 0.5 mM phenylmethylsulfonyl fluoride, 1 mM DTT) containing 100 mM KCl. After removal of insoluble material by centrifugation, the soluble fraction was used for GST pull-down assays.

GST pull-down assays. Ten microliters of glutathione-Sepharose 4B (Amersham Pharmacia Biotech) was equilibrated with buffer C containing 100 mM KCl and 0.1% Triton X-100 and was incubated with *E. coli* extract containing a GST-fusion protein at 4°C for 1 h. The quantity of each *E. coli* extract was adjusted so that an equal amount of GST fusion proteins could be retained on the resin. In all assays, each GST fusion protein immobilized on glutathione-Sepharose 4B was analyzed by sodium dodecyl sulfate-polyacrylamide gel electrophoresis (SDS-PAGE) to ensure that essentially the same amount of GST fusion proteins was immobilized on each resin. After extensive washing of the resin with the same buffer, either 200 ng of recombinant TFIIH or 240 ng of FLAG-tagged GAL4-VP16 was added to the resin suspended in 100 μl of buffer C, and the mixture was incubated at 4°C for 1 h with constant rotation. After the resin had been washed extensively with the equilibration buffer, the bound proteins were eluted with 10 μl of buffer C containing 1 M KCl and 0.1% Triton X-100. Two microliters of each eluate was separated by SDS–12% PAGE and detected by Western blotting with anti-FLAG M2 antibody (Sigma).

Phosphorylation of PC4-GST. Fifty micrograms of PC4-GST immobilized on 10 μl of glutathione-Sepharose 4B was phosphorylated in reaction mixtures (200 μl) containing 20 mM Tris-HCl (pH 7.5), 50 mM KCl, 10 mM $MgCl_2$, 0.2 mM ATP, and 50 U of casein kinase II (New England Biolabs)/μl at 30°C for 1 h. Phosphorylation of PC4-GST was confirmed by both radiolabeling with [γ-^{32}P]ATP and the mobility change on a SDS–15% polyacrylamide gel.

DNase I footprint assays. The promoter regions that contained GAL4 sites were PCR amplified from pG1HMC2AT, pG3HMC2AT, and pG5HMC2AT by using the primers 5′-GTAAAACGACGGCCAGT-3′ and 5′-CCGGGGATCC GGGGATGAGAGTGAATGATGATAGATTTG-3′. After digestion with EcoRI and BamHI, the PCR fragments were subcloned between the EcoRI and BamHI sites of pUC19 to create pUC19-G1, pUC19-G3, and pUC19-G5, which were then entirely sequenced to rule out the possibility of spurious mutations. The plasmids were digested with PvuI and XbaI, and the DNA fragments containing GAL4 sites were isolated after separation on a 4% polyacrylamide gel. Four picomoles of the DNA fragments were labeled by Klenow fragment (New England Biolabs) by using 50 μCi [α-^{32}P]dCTP. Each labeled DNA fragment was then diluted with the same unlabeled fragment to obtain ~2×10^4 cpm per 24 femtomoles of each fragment.

DNA binding reaction mixtures (25 μl) contained 12 mM HEPES-KOH (pH

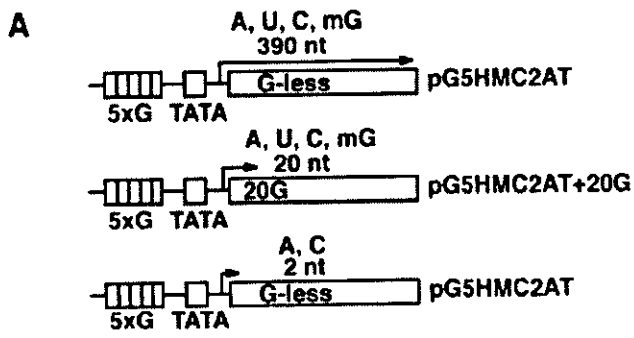

C

Transcript	Fold Stimulation	
	+GVP	+GVP, +PC4
2 nt	2.1	3.2
20 nt	3.0	13.0
390 nt	3.5	16.6

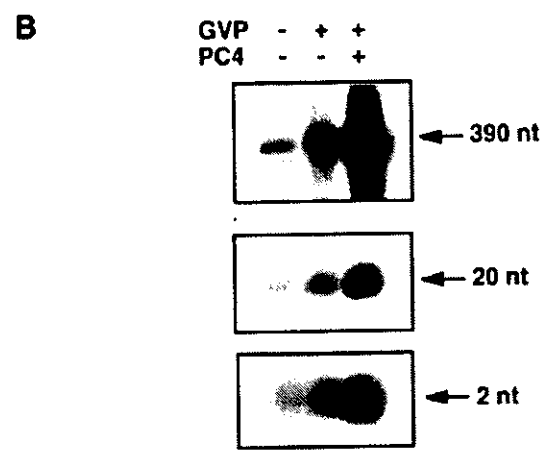

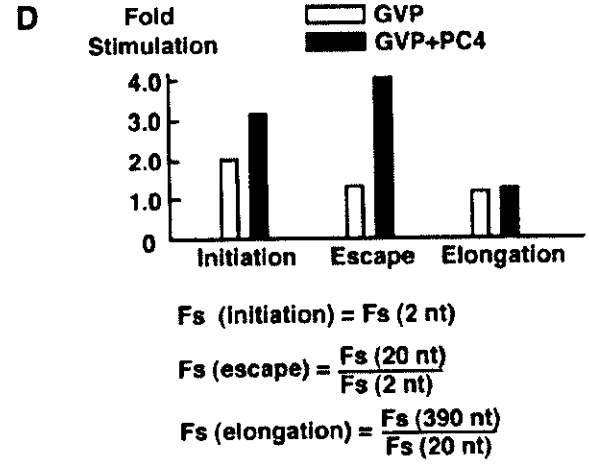

FIG. 1. Effect of PC4 on promoter escape. (A) DNA templates used for in vitro transcription analyses. The template pG5HMC2AT contains five GAL4-binding sites upstream of the human immunodeficiency virus TATA box and the initiator from the Ad2 ML promoter fused to a 380-bp G-less cassette. This template produces the 390-nt transcript in the presence of ATP (A), CTP (C), UTP (U), and 3′-*o*-methyl GTP (mG) and the 2-nt transcript (initiation product) in the presence of ATP and CTP. The template pG5HMC2AT+20G, which is identical to pG5HMC2AT except that it contains a guanine residue at the +20 position, produces the 20-nt transcript in the presence of ATP, CTP, UTP, and 3′-*o*-methyl GTP. (B) Effect of GAL4-VP16 and PC4 upon the 390-, 20-, and 2-nt transcripts. All transcription reactions contained general transcription factors (TFIIA, TFIIB, TFIID, TFIIE, TFIIF, and TFIIH) and RNAPII in the presence or absence of GAL4-VP16 and PC4. The transcripts were separated on a denaturing polyacrylamide gel and autographed. (C) The levels of stimulation (*n*-fold) for the 2-, 20-, and 390-nt transcripts. The transcripts were quantified by using Fujix Bas 2000, and stimulation (*n*-fold) was determined for transcripts in the presence of GAL4-VP16 or GAL4-VP16 and PC4 by using the level for the transcript in the absence of GAL4-VP16 and PC4 as the basal level of transcription. (D) Fold stimulation (Fs) for each step of transcription was determined as indicated by using the values of Fs for the 2-, 20-, and 390-nt transcripts shown in panel C. Open bars indicate Fs in the presence of GAL4-VP16, whereas closed bars indicate Fs in the presence of GAL4-VP16 and PC4. For example, a value of 4.1 for Fs (escape) in the presence of GAL4-VP16 and PC4, indicated by a closed bar above "Escape" in the bar graph, was obtained by dividing of Fs (20 nt) (13.0) by Fs (2 nt) (3.2) in the presence of GAL4-VP16 and PC4.

7.9), 6% glycerol, 60 mM KCl, 0.6 mM EDTA, 8 mM $MgCl_2$, 5 mM DTT, the indicated amount of GAL4-VP16, and 24 fmol of the labeled fragment and pUC19, which corresponds to approximately 50 ng of pG5HMC2AT used for in vitro transcription reactions. The reaction mixtures were incubated at 30°C for 60 min, and the DNA fragment was digested with DNase I for 2 min at room temperature by adding 25 μl of 5 mM $CaCl_2$–10 mM $MgCl_2$ containing 0.002 U of DNase I (TaKaRa). The DNase I digestion was stopped by adding 150 μl of stop solution (0.2% SDS, 20 mM EDTA), 20 μg of glycogen, and 5 μg of proteinase K, and the reaction mixtures were further incubated at 37°C for 60 min. After extraction with phenol and chloroform, the DNA fragment was precipitated with ethanol and rinsed twice with 70% ethanol. The dried pellet was redissolved in 2 μl of 90% formamide–0.025% (wt/vol) xylene cyanol and separated on a 4% denaturing polyacrylamide gel.

RESULTS

Promoter escape is a target for the coactivator activity of PC4. To gain a mechanistic insight into the coactivator function in transcriptional activation, we utilized a model in vitro transcription system that included GAL4-VP16 as an activator and PC4 as a coactivator. This in vitro transcription system contained well-defined components, including recombinant factors (TFIIA, TFIIB, TFIIE, TFIIF, TFIIH, PC4, and GAL4-VP16) as well as highly purified HeLa cell-derived FLAG-tagged TFIID and RNA polymerase II (10–12), and exhibited marked transcriptional activation in response to GAL4-VP16 in a highly PC4-dependent manner. These features of this system provided an excellent opportunity to analyze mechanistic aspects of the coactivator function of PC4 in a quantitative manner.

To accurately quantify the effects of PC4, we focused exclusively on measuring the amounts of the 2-, 20-, and 390-nt transcripts (Fig. 1A). We took this approach because measuring the amount of PIC (either by immunoblotting or by gel-mobility shift) and the degree of promoter opening (by potas-

sium permanganate footprinting) did not give sufficiently accurate values compared to measuring the amounts of transcripts and therefore did not provide useful information for detailed quantitative analyses. For this reason, the effects of PC4 on PIC assembly and promoter opening are subsumed in the effects on the 2-nt ApC formation, which corresponds to the initiation step on the templates used in this study (Fig. 1A). Accordingly, unless otherwise stated, the term "initiation," used hereafter for brevity, includes all three steps: PIC assembly, promoter opening, and ApC formation.

Using this reconstituted in vitro transcription system, we measured the levels of the 2-, 20-, and 390-nt transcripts produced from the template pG5HMC2AT or its derivatives (Fig. 1A). The 2-nt initiation transcript, which is ApC on the template pG5HMC2AT, was produced in the presence of ATP and CTP. The 20-nt transcript was produced in the presence of ATP, CTP, UTP, and 3′-*o*-methyl GTP from template pG5HMC2AT+20G, which contained a G residue at the +20 position, at which transcription terminates through incorporation of 3′-*o*-methyl GTP (Fig. 1A). The 390-nt transcript was produced from template pG5HMC2AT in the presence of ATP, CTP, UTP, and 3′-*o*-methyl GTP. After the relative amounts of these transcripts had been determined, the effects of GAL4-VP16 or GAL4-VP16 and PC4 on initiation, promoter escape, and elongation were estimated (Fig. 1B and C). The effect on initiation was estimated directly from the stimulation (*n*-fold) of the 2-nt transcript. Also, the effect on promoter escape was estimated by dividing the stimulation (*n*-fold) of the 20-nt transcript by that of the 2-nt transcript, and likewise, the effect on elongation was estimated by dividing the stimulation (*n*-fold) of the 390-nt transcript by that of the 20-nt transcript.

As shown in Fig. 1B and C, GAL4-VP16 alone stimulated the production of the 2-, 20-, and 390-nt transcripts 2.1-, 3.0-, and 3.5-fold, respectively. Thus, the effects of GAL4-VP16 on initiation, promoter escape, and elongation were calculated as 2.1-, 1.4-, and 1.2-fold, respectively, indicating that GAL4-VP16 stimulated mostly initiation and had lesser effects on promoter escape and elongation (Fig. 1D). Further inclusion of PC4 in these reactions stimulated the production of the 2-, 20-, and 390-nt transcripts 3.2-, 13.0-, and 16.6-fold, respectively (Fig. 1C). Thus, the combined stimulatory effects of GAL4-VP16 and PC4 on initiation, promoter escape, and elongation were 3.2-, 4.1-, and 1.3-fold, respectively, indicating that PC4 augments the ability of GAL4-VP16 to stimulate initiation, promoter escape, and, to a lesser degree, elongation (Fig. 1D). It is notable that the effects of PC4 on the coactivation of GAL4-VP16 are more pronounced at the promoter escape step than at the other steps (Fig. 1D). Taken together, these results not only corroborate a previous demonstration that PC4 acts through the facilitated PIC assembly (13, 21) but also highlight promoter escape as yet another step facilitated by the coactivator activity of PC4.

PC4 requires TFIIA and TAFs for stimulating promoter escape in response to GAL4-VP16. Previous biochemical studies demonstrated that TFIIA and the TAF subunits of TFIID greatly enhance transcriptional activation in vitro. Despite the well-documented roles of TFIIA and TFIID during the assembly of PIC (7, 8, 24, 33), their effects on promoter escape in activated transcription remain undefined. Moreover, observations that TBP alone supports transcriptional activation by various activators, including GAL4-VP16 (39, 43, 59, 64), suggest that some steps may be stimulated without TAFs.

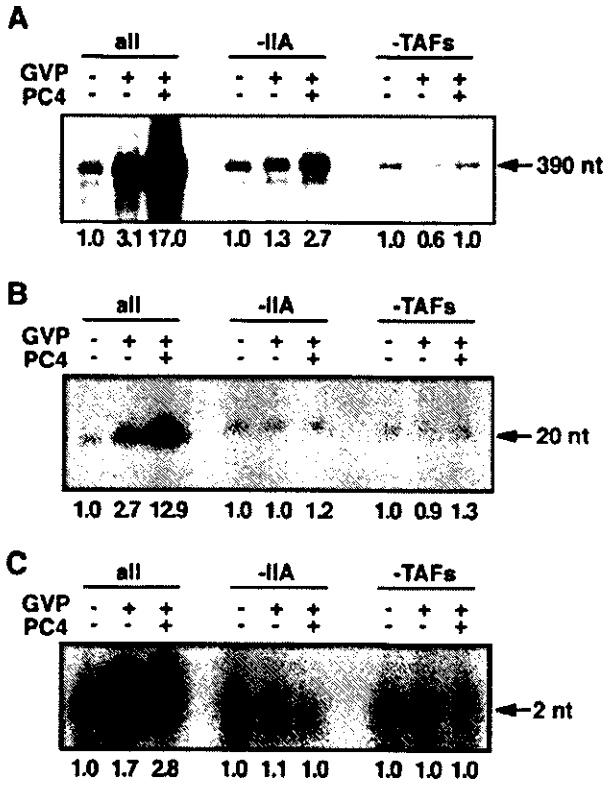

FIG. 2. Requirement of TFIIA and TAFs for stimulation of promoter escape by PC4. Stimulation of the 390-nt (A), 20-nt (B), and 2-nt (C) transcripts in the absence of TFIIA or TAFs. Transcription reactions were done in the absence of TFIIA (−IIA) or the TAF subunits of TFIID by using pG5HMC2AT or pG5HMC2AT+20G. The levels of stimulation of each transcript (*n*-fold) are indicated below the autoradiograms of the gels. In the absence of TFIIA or TAF subunits of TFIID, little stimulatory effect was observed on initiation, promoter escape, and elongation in the presence of GAL4-VP16 or in the presence of both GAL4-VP16 and PC4 except for a small stimulatory effect (i.e., ~2.3-fold) on elongation by PC4 in the absence of TFIIA, an effect that was dependent upon the presence of TFIID.

To determine whether TFIIA and TAFs are required for mediating the stimulation of promoter escape by GAL4-VP16 and PC4, we performed in vitro transcription assays in the presence or absence of TFIIA and TAFs. When TFIIA was removed from the reactions, the 2-, 20-, and 390-nt transcripts were stimulated 1.1-, 1.0-, and 1.3-fold, respectively, in the presence of GAL4-VP16 alone and 1.0-, 1.2-, and 2.7-fold, respectively, in the presence of GAL4-VP16 and PC4 (Fig. 2). Thus, in the absence of TFIIA, there was little stimulation of initiation and promoter escape by PC4 in response to GAL4-VP16. Interestingly, an approximately twofold stimulatory effect on elongation by GAL4-VP16 and PC4 remained intact even in the absence of TFIIA, albeit in a TAF-dependent manner (Fig. 2A and B), although this effect was not pursued further in this study. When TFIID was replaced by TBP, the 2-, 20-, and 390-nt transcripts were stimulated 0.6-, 0.9-, and 1.0-fold, respectively, in the presence of GAL4-VP16 and 1.0-,